LAPPEENRANTA UNIVERSITY OF TECHNOLOGY
LUT SCHOOL OF ENGINEERING SCIENCE
DEGREE PROGRAMME OF CHEMICAL AND PROCESS ENGINEERING

Petrus Suokas

FRACTIONATION OF TAILINGS

Examiners: Professor, D.Sc. Antti Häkkinen
Post-Doc Researcher, D.Sc. Riina Salmimies
Supervisor: Senior scientists, PhD Antti Grönroos

ABSTRACT

Lappeenranta University of Technology
LUT School of Engineering Science
Degree programme of Chemical and Process Engineering

Petrus Suokas

Fractionation of tailings

Master's Thesis, 2016
75 pages, 27 figures, 22 tables and 3 appendices
Examiners: Professor, D.Sc. Antti Häkkinen
Post-Doc Researcher, D.Sc. Riina Salmimies
Keywords: Tailings, dewatering, fractionation, hydrocyclones

Mining industry produces vast amounts of tailings which are categorized as waste products even though they may still contain lots of valuable metals that could be extracted. Metals that are carried along with the tailings to tailing dams can be found from different sized particles which can be recovered after they have been identified. Hydrocyclones are commonly used in mining industry for separation of different particle size fractions from each other in economic way and for the concentration of the tailings slurries.

The target of this thesis is to determine the fractionation efficiency of a laboratory-scale hydrocyclone. The effect of geometrical dimensions of the hydrocyclone is studied by changing the sizes of the vortex finder orifice and underflow spigot. The changes in fractionation efficiency of the solid particles of the tailings are detected by solid concentration and particle size distribution analyses which are studied from both over and underflows. Vortex finder orifices that are used in this study have diameters of 14 mm, 11 mm and 8 mm. Underflow spigots that are used have outlet diameters of 8 mm, 6 mm, 5 mm and 3 mm.

TIIVISTELMÄ

Lappeenrannan teknillinen yliopisto

LUT School on Engineering Science

Kemiantekniikan maisteriohjelma

Petrus Suokas

Rikastushiekan fraktiointi

Diplomityö, 2016

74 sivua, 27 kuvaa, 22 taulukkoa, 3 liitettä

Tarkastajat: Professori, TkT Antti Häkkinen

Tutkijatohtori, TkT Riina Salmimies

Avainsanat: Rikastushiekka, fraktiointi, hydrosykloni, vedenpoisto

Kaivosteollisuus tuottaa vuosittain maailmanlaajuisesti valtavan määrän rikastusprosessin ohessa syntyvää rikastushiekkaa. Vaikka rikastushiekka luokitellaan jätteeksi, joutuu sen mukana runsaasti metalleja varastoaltaisiin. Metallit jotka joutuvat rikastushiekan mukana jätealtaisiin voitaisiin saada talteen, sillä metallijäämien tiedetään rikastuvan tiettyihin partikkelikokojakeisiin. Tunnistamalla nämä partikkelit ja erottamalla ne muusta jätehiekasta metallit pystyttäisiin keräämään talteen. Hydrosykloneita käytetään yleisesti kaivosteollisuudessa erikokoisten partikkelien luokitteluun ja erottamiseen toisistaan sekä jätealtaisiin pumpattavan jätteen konsentrointiin.

Työn tavoitteena on tutkia hydrosyklonin erotuskyvyn muuttumista muuttamalla sen geometrisia suhteita. Geometristen mittasuhteiden muuttaminen tapahtuu muuttamalla hydrosyklonin ylite- ja aliteaukojen kokoa. Erotuskyvyn muutosta tutkitaan sekä ylitteen että alitteen partikkelikoko- sekä kiintoainepitoisuusanalyyseilla. Kokeissa käytetyt yliteaukkojen koot olivat 14 mm, 11 mm, ja 8 mm ja aliteaukkojen koot olivat vastaavasti 8 mm, 6 mm, 5 mm sekä 3 mm.

NOMENCLATURE

D_c	Diameter of hydrocyclone	(m)
D_i	Diameter of the feed inlet	(m)
D_o	Diameter of the overflow orifice	(m)
D_u	Diameter of the underflow orifice	(m)
E_T	Total separation efficiency	(%)
F_x	Mass fraction of particles of size x in the feed	(w-%)
$F_{u,x}$	Mass fraction of particles of size x in underflow	(w-%)
$F_{o,x}$	Mass fraction of particles of size x in overflow	(w-%)
G(x)	Grade efficiency	(-)
G´(x)	Reduced grade efficiency	(-)
M	Total mass flowrate	(kg m^{-1}h)
M_u	Recovered mass of coarse material in underflow	(kg)
M_o	Recovered mass of fine material in overflow	(kg)
n	Hydrodynamic constant	(-)
Q	Total volumetric flow rate	(m^3 s^{-1})
Re	Reynolds number	(-)
R_f	Feed ratio of flows	(-)
Stk	Stokes umber	(-)
Stk_{50}	Stokes number for cut size particles	(-)
v	Flow velocity of the feed	(m s^{-1})
x	Particle size	(m)
x_{50}	Cut size	(m)
x'_{50}	Reduced cut size	(m)

Δp	Pressure drop	(N m^{-2})
ρ	Density of liquid	(kg m^{-3})
ρ_s	Density of solids	(kg m^{-3})
τ	Particle relaxation time	(s)

ABBREVIATIONS

AMD	Acid mine drainage
DITR	Department of Industry, Tourism and Resources
LZVV	Locus of zero vertical velocity line
OF	Overflow
STDdev	Standard deviation
UF	Underflow
(w/v)	Mass/volume

Table of Contents

LITERATURE PART

1 INTRODUCTION

Mining industry creates vast amounts of tailings which are commonly stored in huge outdoor ponds where they are let to settle and in some cases the clarified water is recycled back to process to reduce the total water consumption. Almost in every process the recovery of metals is never complete and some valuable minerals remain in the tailings. In order to recover these valuable metals, such as cobalt, copper and nickel, tailings need to be treated in one way or another. The recovery of these valuable metals can be done by leaching which is done after fractionation and dewatering of the tailings. Fractionation is an important phase as it allows the separation of the particles which are not important in further processing. Pre-treatment also plays an important role in reducing the amount of overall tailings waste created and impact caused to the surrounding environment of the mine.

The main focus of this thesis is to investigate the possibility to concentrate and fractionate metal ore tailings with hydrocyclone. Different sets of operating and design parameters, such as feed pressure and orifice sizes will be used in order to obtain an overall understanding of the most important parameters effecting on the fractionation efficiency.

2 TAILINGS

Tailings are a side product of all ore beneficiation processes. They are composed basically of water and gangue, but they may also contain chemicals originating from the process and even some valuable metals that have not been recovered from the metal ore.

Majority of the mass of the ores processed ends up in tailings because the valuable mineral commonly represents only a small percentual fraction of the total rock mass handled. After the beneficiation of the mineral and recovery of the wanted metals, the remaining rock is carried into tailings. For example in gold mines the mass fraction of the waste rock can easily be over 99% due to the commonly low concentrations of gold in the ore (Lottermoser 2010).

Davies (2011) has divided tailings into two categories which are either pumpable or non-pumpable tailings. Pumpable tailings consist of non-treated slurries, thickened tailings and pastes and the transportation of these is typically done by pumping. Non-pumpable tailings are wet or dry cakes. Non-pumpable tailings are transported to the storage area by conveyor belts or by trucks. The categorization is illustrated in Figure 1 which also represents the chain of tailings treatment from the point of water removal and total volume reduction.

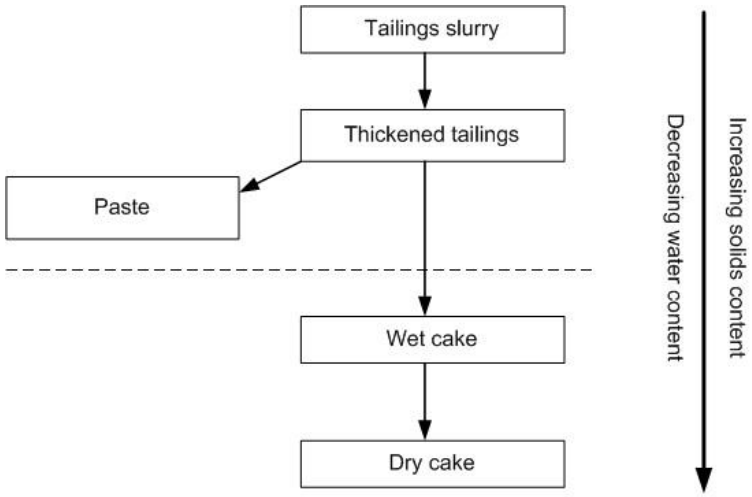

Figure 1 The categorization and treatment chain of tailings. Pumpable slurries which take most space in the storage areas are located above of the dividing line and non-pumpable tailings which take less space due to reduced water content are located under the line (after Davies, 2011).

2.1 Composition of tailings

The composition of tailings varies between sites due to the processes used and ores beneficiated and therefore there is no universal classification for the tailings based purely on their constituents. Tailings are composed of water, gangue, some chemicals and residue metals which have not been recovered from the ore. Reason for this can be for example that the metal is located inside the ore lattice and it is not extracted because of this in the beneficiation process (Lutandula and Maloba, 2013; Andrews *et al*., 2013). If the amount of metals inside the tailings is large enough, and the extraction process would be beneficial, the tailings could be re-treated with suitable processes to separate and collect the valuable metals from tailings (Lottermoser, 2010).

Tailings have different kind of solid contents varying from very low solid content to over 80 w-% of solids and they can be divided roughly into three categories: slurries, thickened slurries/tailings and dewatered tailings. Slurries have the lowest solid content being typically ≤ 50 w-%. Slurries can go through a water removal process which increases the solid content, but commonly they are pumped without any treatment to storage sites. Thickened tailings go through water removal process and their solid content can be up to 80 w-%. Dewatered tailings have the highest solid content as they go through a water removal process which removes most of the water from tailings producing cakes. Dewatered tailings often have solid contents over 80 w-% (Franks *et al*., 2011; DITR, 2007; Lottermoser, 2010).

The chemical composition of tailings varies between sites as the composition depends on the type of the original ore and the processes used to recover the wanted metal(s). Generally all tailings contain chemical residues from the extraction process, products of chemical reactions taking place inside the tailings, dissolved metals and waste rock. Zagury *et al*. (2004) studied the metal composition of fresh and aged mine tailings with samples taken from 1 meter depth. The metal composition can be seen in Table I.

Table I Metal composition of mine tailings (Zagury *et al*., 2004)

Metal	Fresh sample [mg/kg]	Aged sample [mg/kg]
Al	5000	8900
Cd	<1	<1
Ca	9100	12000
Co	13	17
Cu	450	930
Fe	42000	53000
Pb	28	20
Ni	5,9	9
Ag	<10	<10
Zn	91	220

As seen on Table I, the concentration of metals change during time. The changes and difference in the chemical composition between fresh and aged tailings could be explained by chemical reactions happening in the tailings, pH changes, constant changes in weather conditions and constant supply of fresh tailings to pond. Table

I shows also that some metals can have relatively high concentrations in tailings after the beneficiation process. In cases of valuable metals this could encourage for further processing of tailings in order to increase the total yield of the process. Processing of tailings could also reduce the overall amount of heavy metals or hazardous chemicals (Adams and Lloyd, 2008).

As the chemical composition of tailings can be complex, the environmental aspects need be taken into account when considering the management and storage of tailings. One of the most significant environmental challenges in mine tailings is acid mine drainage (AMD). Acid mine drainage is the result of oxidation of sulfate minerals and ores and it accelerates the leaching of metals and affects the solubility of metals in gangue and waste waters. The release of heavy metals inside tailings ponds is strongly related to the changes which occur in the pH of the waste water. (Lottermoser, 2010; Johnson and Hallberg, 2005).

3 TREATMENT AND STORAGING OF TAILINGS

Treatment methods consist usually from the processes which target at reducing the water content of the tailings and they are commonly used throughout the mining industry. Especially in the arid regions where water is a scarce resource, the dewatering of tailings improves the water economy of the plant since the excess water from tailings can be recycled back to the process (Gunson *et al*., 2012). It also generally reduces the overall environmental impact of ore processing by reducing the raw water consumption. By removing the surplus water from tailings, the storage space needed for storing them can be drastically reduced as the main substance that is deposited to storage facilities is solids instead of water. This can lead to smaller tailings storage facilities or extend the lifespan of these facilities (Lottermoser, 2010). Treatment of tailings can also include chemical adjustments. These processes can include pH adjustments in order to prevent heavy metal dissolution to the tailings water, neutralization of the tailings in order to prevent AMD and recovery of the chemicals used in the process (Adams and Lloyd, 2008; Davies, 2011; Heiskanen, 1987).

3.1 Dewatering and desliming of tailings

Due to the increased environmental awareness and tightening legislations concerning environmental aspects and influence of mines and mining industry to the environment, numerous books, reviews and studies have been made to improve the overall effectiveness of mines and to reduce their environmental impact from the point of water economy and effectiveness (Johnson and Hallberg, 2005, Franks *et al,* 2011.; Ritcey, 2005). It is known that metallurgical processes use large amounts of water. For example, a plant without recycling of the process water can consume up to 3,0 m^3 of water per ton of ore. This is one of the reasons why nowadays most plants have at least some kind of recycling of the process waters. To improve the water efficiency of a plant, dewatering and desliming processes are considered to be in big role (El-Shall and Zhang, 2004; Gunson *et al*., 2012, Lottermoser, 2010, Yan *et al*., 2002).

Dewatering of tailings is one of the treatment methods used for tailings. It is an effective way to reduce the amount of depositable tailings waste and in general allows the collection and recycling of the surplus water and possible chemicals back to the process. The general idea is to remove excess water from the tailings slurries to increase the solid content. Depending on the wanted solid content level, the products are thickened slurries, pastes or cakes. The equipment used for dewatering also depends on the wanted solid content on the product. For thickened slurries, thickeners and hydrocyclones can be used to achieve the wanted levels. For drier products, different kinds of filters (drum- and belt filters) are commonly used (Davies, 2011; DITR, 2007; Lottermoser, 2010).

Usually the dewatering and treatment of tailings is done from the point of coarse faction of solids as they are easier to handle rather than the fine fraction of solids. When the process considers the removing of fine/ultrafine particle section the process is called desliming (Kesimal *et al*., 2003). The presence of fine particles in the system can cause various problems in waste handling and in the beneficiation process. These can appear in forms of clogging of filtration media, impairment of filtration, increased retention and sedimentation times of slurries and for example in case of cemented backfilling in form of reduction in structural integrity (Galvin *et al*., 2012; Ercikdi *et al.*, 2013). In the desliming process the used equipment is

generally same as in dewatering in addition centrifuges can be used as they are effective in separation of fine particles (Batalovic, 2011).

As said, the fine particles cause numerous troubles on the process in many ways. One of them is the increased sedimentation time in thickeners and tailing bonds, which results in longer retention time of tailings storage facilities. To reduce the sedimentation time flocculants and/or other binding media can be used. A study done by El-Shall and Zhang (2004) studied the effect of flocculants accompanied with binding material in order to reduce the sedimentation time of very fine particles and the effect of this combination in dewatering of these solids. The particle size distribution of the tailings sample used is represented in Table II.

Table II Particle size distribution of the sample (El-Shall and Zhang, 2004)

Size [µm]	Cumulative weight Passing [%]
17,99	90
9,41	75
4,73	50
2,39	25
0,49	10

To enhance sedimentation El-Shall and Zhang (2004) studied the effect of three different anionic flocculants in the process by making a solution containing 0,05 w-% of the chosen flocculants which were added to the slurry. Flocculants used were Percol 156, Nalco 7877, Arrmaz 856 and Arrmaz 957. As a binding material, newspaper fiber was used. Sedimentation tests were carried out by mixing a wanted amount of fibers with the slurry and adding fixed amount of flocculants to the solid-fiber mixture followed by inverting the vessel for ten times after the mixture was let to settle and the height of the descending interface was recorded. Filtration tests were carried out with adding flocculants to the slurry and filtering the mixture in with a Buchner funnel and the amount of filtrate was recorded. The filtration results from the vacuum filtration can be seen from Table III.

Table III Results for fixed amount of filtrate to be obtained from the Buchner vacuum filter using 3 ppm solution of Percol 156 (El-Shall and Zhang, 2004)

	Time [s]	
Filtrate volume [mL)]	Fiber 0 w-%	Fiber 5 w-%
10	6	6
20	18	14
30	29	20
40	42	24
50	56	31

Vacuum tests indicated that adding fiber lowered the filtration time of the samples, but when the fiber content was more than 10 w-% the fibers impede the filtration due to the blinding of the filter media and filtration speed reduces. Low levels of fibers were in the other had noticed to form a layer which prevents the fine particles in the slurry to blind the filter media.

Dewatering tests were carried out by making samples of slurry with and without added paper fibers added with 3 ppm Percol 156 solution. After the creating of the sample 200 ml was poured on the plastic screen where slurry was let to remain for one minute during which the water and solids passing the screen was measured. Results from the screening test showed that if the fiber media was not added to the slurry, about 50% of the flocculated clays went through the screen. This indicated that adding fibers to the slurry the flocs were strengthened allowing more solids to be caught in the screen. Also the addition of fibers increased the retention time increasing the solids recovery and made it possible to add a pressing stage to the dewatering process.

From the results obtained from the tests small scale pilot plant was created. Flowchart of the pilot plant is shown in Figure 9. Pilot plant contained same stages as performed tests. Because of the poor results from vacuum filtering the stage was removed and one additional screen and belt press was implemented to the system.

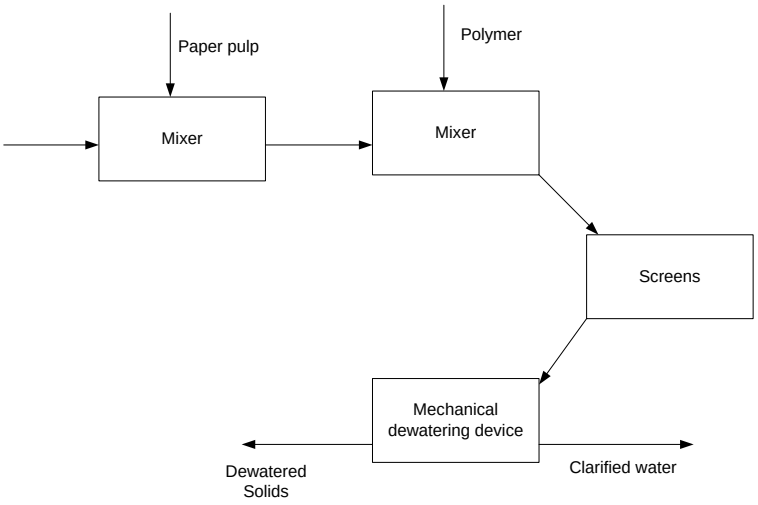

Figure 2 Flowchart of the pilot plant (after El-Shall and Zhang, 2004)

For the pilot plant tests a combination of slurry containing 6 w-% of fibers and 5 ppm of Nalco 7877 flocculant was selected. The results of pilot plant tests are shown in Table IV.

Table IV Results from pilot plant tests using 6 w-% of fibers and 0,5 kg/t flocculant (El-Shall and Zhang, 2004)

	Solids in product [w-%]		
Solids in feed [w-%]	First Screen	Second screen	Belt press
3	16	20	45
4	14	19	50
5	14	21	48
6	24	32	47

The results indicate that adding fibers or other filter aids and inducing a pressing stage to the process make it possible to achieve the wanted moisture level of cake when dewatering tailings rather easily and with small effort. In addition with reduced moisture levels in cake the filtrate was clearer and free from visible particles.

3.2 Storing facilities and methods for tailings

The purpose for disposal facilities is to contain all the waste produced from the ore beneficiation process and separate them from the surrounding environment. As the material flows are vast in mineral processing the disposal sites are commonly very large in size and have strong impact on the surrounding environment in geological

and esthetical way. In addition disposal facilities create a risk of chemical contamination of the ground and ground water through the seepage waters as the might contain Process chemicals, heavy metals or may have alkaline or acidic nature (Lottermoser, 2010; DITR, 2007).

3.2.1 Above ground facilities

The most common way to deposit tailings is to pump them in large surface impoundments called tailing dams. The purpose of these impoundments is to store all tailing waste produced in beneficiation process and isolate them from the surrounding environment. To prevent the seepage the tailing the inner walls and bottom of the dam are coated with waterproof liner. In addition clay or other soil with very low water penetration ability can be used in the foundations. Tailings are pumped to these ponds as low-concentration or thickened slurry. In the ponds stable layers of solids form through settling. Water separates as its own phase on top of the solids and can be collected and recycled back to the process if so wanted. The level of water inside ponds is controlled by recycling it back to process or releasing it back to the surrounding environment if the water is pure enough. Releasing of the water back to environment may need additional settling pond where the water is let to further clarify. The simplified crosscut sketch is of the tailing dam is illustrated in Figure 3 (Lottermoser, 2010; Martin et al., 2002; Will's, 2007).

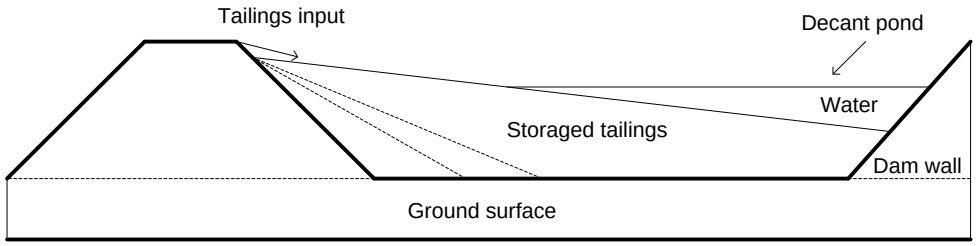

Figure 3 Simplified picture from tailing dam structure (after Lottermoser, 2010).

The above-ground facilities can be built on flat ground or the facility can be built in ways that it uses the existing ground topography, for example valleys or existing mine pits in their advantage. The tailings deposit facilities grow in hand-to-hand with the amount of tailings pumped to the pool. Walls of the ponds are heightened when the level of tailings inside point reach their limit. Materials used in the heightening of the walls can be rock, sand and even tailings. The use of tailings as

construction material is determined by their chemical and physical properties. Tailings consisting hazardous materials cannot be used since may cause hazardous leaking to the environment (Lottermoser, 2010; Martin *et al*., 2002; Will's, 2007)

Drystacked tailings are dewatered to the stage where their physical appearance resembles wet or dry sand more than slurry and therefore their disposal facilities differ from the storage facilities of slurries and pastes. Drystacking is an effective way to store tailings as the requirements for the storing area is reduced along with the reduced tailings volume. Drystacking is favored especially in warm and arid areas where water is a scarce resource. In these cases tailings are dewatered and the water is recycled back to the process (Davies, 2004; Davies, 2011; Lottermoser 2010).

In backfilling the slurry is commonly concentrated either to paste or to dry cakes. After the dewatering the remaining tailings waste is pumped for example into old mine pits or underground mine tunnels where it is deposited. This method reduces the need for construction of tailing ponds but it has drawbacks as the ground water level rises back to the pre-mining level. This causes deposited tailings to come into contact with water and cause formation of AMD and lead to the release of heavy metals and chemicals to the groundwater and may pollute the surrounding water system. To prevent possible chemical and heavy metal leakages the tailings can be treated with cement to stabilize their structure and prevent the dissolution of metals and chemical traces) or the deposit place can be coated with protective layer (Choi *et al*., 2009, El-Shall and Zhang, 2004, Lottermoser 2010).

Choi *et al*. (2009) stabilized non-treated tailings samples from three different tailings storage sites (A,B,C) and studied the effect of stabilization with cement to the leachability of Ar, Cd, Pb and Zn metals. Three set of different methods was used in the leaches: Korean standard leaching test (KSLT), synthetic precipitation leaching procedure (SPLP) and toxicity characteristics leaching (TCLP). Leaches were done three times in order to ensure the repeatability of the tests with 1 N HCl solution. The results from non-cemented leaching of the samples with 1 N HCl are represented in Table V.

Table V Results for the leaching tests including deviation between tests, particle size analysis and water content for the non-treated tailings (Choi *et al*., 2009).

Tailing source	As [mg/kg]	Pb [mg/kg]	Cd [mg/kg]	Zn [mg/kg]	d_{10} [mm]	d_{60} [mm]	Water content [w-%]
A	88,2±10,7	3,35±0,29	0,053±0,003	3,46	0,075	0,19	4,7
B	1,39±1,22	4,04±0,18	0,026±0,003	4,03	0,85	4,75	5,0
C	73,3±26,6	34,9±1,53	0,006±0,004	1,55	0,085	0,23	5,0

From the results can be seen that two of the samples, A and B gave very high arsenic leachabilities and in addition to arsenic sample C gave high leachability of lead.

After the results of non-cemented leaching samples of tailings was mixed with Portland cement with concentrations varying from 5 w-% to 30 w-%. After drying for one week the physical integrity of the blocks was tested with compressive strength test. After the compressive test the samples were leached with the three different leaching methods, KSLT, SPLP and TCLP. The results of the KSLT is represented in the table VI. Results from the other two leaching test were very similar with the KSLT results.

Table VI Leaching results for the raw mine tailings and their stabilized forms from KSLT test (*Choi et al*., 2009)

		Cement content [w-%]							
Tailing source	Metal [mg/L]	0	5	7,5	10	15	20	25	30
A	As	1,14	0,08	0,01	0,001	0,002	0,002	0,002	0,001
	Pb	0,4	0,07	0,03	0,06	0,004	0,03	0,03	0,085
	Cd	0,01	nd[a]	0	0,001	0,002	0,003	0,003	0,004
B	As	0,03	nd[a]	nd[a]	nd[a]	nd[a]	nd[a]	nd[a]	nd[a]
	Pb	0,27	0,08	0,05	0,07	0,07	nd[a]	0,05	nd[a]
	Cd	0,01	nd[a]	nd[a]	nd[a]	nd[a]	nd[a]	nd[a]	nd[a]
C	As	0,73	0,28	0,11	0,01	0,01	0,01	0,004	nd[a]
	Pb	0,41	0,05	0,05	0,1	0,1	0,09	0,07	0,12
	Cd	0,01	nd[a]	nd[a]	nd[a]	nd[a]	nd[a]	nd[a]	nd[a]

[a] Not detected (Limits: As: 0,0004 mg/L Pb: 0,02 mg/L Cd 0,0007 mg/L)

From the results it be seen clearly that the optimal cement content for stabilizing tailings in order to prevent the majority of leaching of metals was 7,5 w-%. Test results shows that when considering the disposal of tailings containing arsenic or

heavy metals stabilizing with cement could be considered. These results support the method of storing tailings as cemented backfill as it can be clearly seen that cementing blocks nearly all of the leaching of the heavy metals.

3.2.2 Riverine, lacustrine and marine disposal

Tailings can be disposed into different kind of water systems. Disposing tailings to the water systems is from the point of environment most harmful way to dispose tailings. Tailings can be carried long distances from the point of release and damage greatly the water systems they are released. Damage is caused from the sedimentation of solids to the bottoms of for example lakes and rivers. Also possible chemicals present in tailings slurry can harm the environment (Lottermoser 2010).

4 TREATMENT EQUIPMENT

Treatment of tailings includes various unit operations like sedimentation and the equipment used is similar as in other fields of industry. The focus in the treatment of tailings is focused mainly to filtration and dewatering equipment. Depending on the site where the treatment is done the equipment used varies. In arid regions where water is scarce resource facilities tend to focus on water removal and dewatering of tailings. This allows recycling the used process water back to the system and reduction for the need of fresh water. Areas where water is abundant resource water recycling can be used in similar way to reduce the need of fresh water and reduce the amount of tailings pumped to tailing dams and so reduce the size of the storing area and the environmental impact caused by it. The commonly used equipment for water removal and thickening of tailings are for example hydrocyclones and thickeners. Hydrocyclones can be used also for classification of the tailings in the purpose of separating different particle fractions from each other. This work is mainly focused in the operation of hydrocyclones.

4.1 Hydrocyclones

Hydrocyclone belong to centrifugal separators as their operating principle is based on the tangential forces created by the swirling motion the suspension receives as the slurry is pumped into the hydrocyclone. The classification range for solids can vary between 2 µm and 500 µm depending on the design of the hydrocyclone.

Hydrocyclones are very adaptable and versatile pieces of equipment which have a wide range of operations. They can operate as solid-solid, solid-liquid and gas-solid separators. Fractionation of same density but different size particles is also possible due to way of the operation of hydrocyclone (Sinnot 2007; Svarovsky, 1984).

Structure of the hydrocyclone is simple and it does not have any moving parts. Prediction of optimal operating conditions is hard because there are multiple interdependent factors influencing the operation of hydrocyclone. Therefore the optimal conditions are usually achieved after field tests and adjustments to the hydrocyclone based on the test results. The parts whence hydrocyclone is constructed are feed inlet, feed chamber, cylindrical upper section, conical lower section and apex (also underflow orifice) Simplified cross-cut picture from the structure of a hydrocyclone and forces present are presented in Figure 4 a) and b) (Firth, 2002; Svarovsky, 1984 and Wills, 2007).

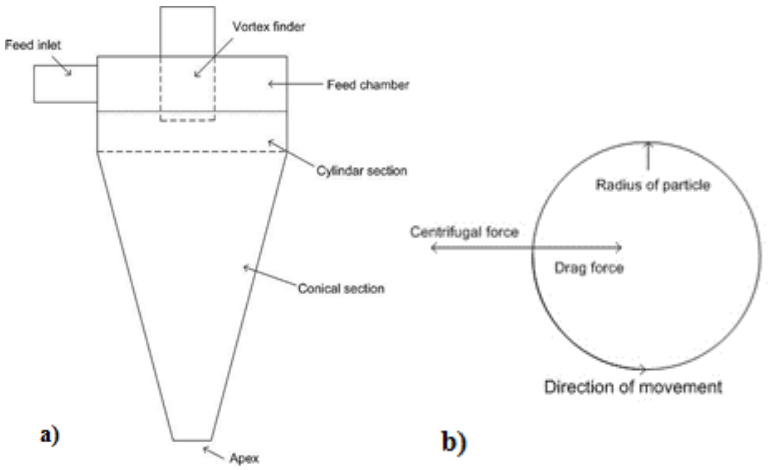

Figure 4 a) Crosscut image from hydrocyclone and its part. b) forces that are affecting the operation of hydrocyclone during operation (After Svarovsky, 1984 and Wills, 2007).

The suspension is pumped from the feed inlet, overflow exits from the top of the hydrocyclone through the vortex finder and the underflow exits through the bottom of the hydrocyclone from underflow apex/orifice. According to Svarovsky (1981; 1984) in order for hydrocylone to be able to operate:

1. There has to be a density difference between the carrying liquid and solids
2. The entering flow has to be steady for the separation to take place
3. Gasses tend to migrate to the middle of the vortex and form gas core inside hydrocyclone

The ability of separation of different fractions from each other is based on the centrifugal and drag forces which are products of tangential, radial and vertical velocities caused from the motion of the suspension and gravity Svarovsky (1981).

Tangential velocity is the velocity that the suspension of liquid and solids gain when they're pumped in. The velocity increases greatly when the suspension is carried downwards the cyclone as the radius of cyclone reduces.

Radial velocity describes the movement of fluid radially inside the hydrocyclone. It is generated by the fact that all of the liquids cannot be carried out vie underflow apex and therefore must be carried out from the vortex finder. This fact creates an inward flow for the liquid, which is at its greatest near the cyclone wall.

Vertical velocity component is essential for the operation of the hydrocyclone as it is the component that removes particles out from the hydrocyclone, but in the other hand it does not take part on the separation of the solids.

4.1.1 Parameters affecting in the operation of hydrocyclone

As Svarovsky (1981; 1984) indicated there are some fundamental issues that must be met before the hydrocyclone may operate as wanted. When the conditions are met, the separation efficiency can be manipulated by adjusting the structural design (Medronho and Coelho, 2001) and operation variables such as pumping pressure and temperature of the suspension (Cilliers *et al.* 2004).

Cilliers *et al*. (2004) studied the effect of the change of temperature to the separation efficiency of the hydrocyclone. The temperature interval was from 10 to 60 ºC. The results indicated that the increase of the suspension from 10 ºC to 60 ºC increased the solids recovery rate by nearly 10 %-units from 72 % to 82% as shown in Figure 5.

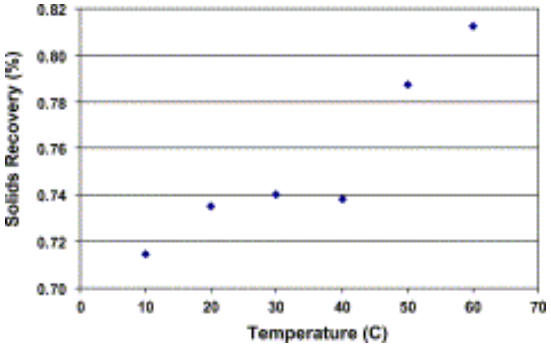

Figure 5 The effect of temperature rise to the solids recovery (Cilliers *et al.*, 2004).

In addition to the solids recovery Cilliers *et al.* (2004) noticed that the increase of temperature reduced the cut size of the hydrocyclone almost to 50 % of the original cut size. The reduction of cut size is illustrated in Figure 6.

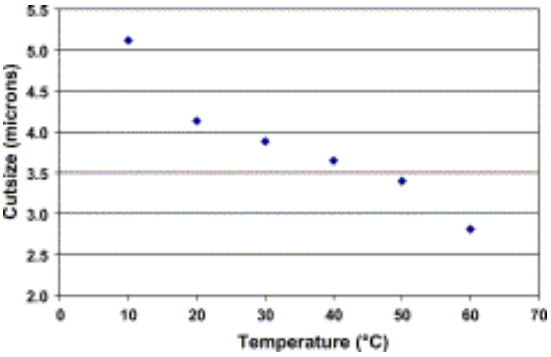

Figure 6 Effect of temperature to the cut size of the hydrocyclone (Cilliers *et al.*, 2004).

The results show that the reduction in water viscosity due to the temperature rise particles face less forces preventing them to move outwards to the outer vortex and be discharged to underflow (Cilliers *et al.*, 2004).

Even more important factors for the operation of hydrocyclone are its design parameters and geometrical proportions. Svarovsky (1984) identifies five design variables that can be changed by adjusting the design of the hydrocyclone. The adjustable properties and the operation needed for the adjustment are shown in Table VII.

Table VII Table of parameter changes needed to adjust the operation of a hydrocyclone (After Svarovsky 1984)

	Adjustment				
Parameter	Increase capacity	Cut size reduction	Improve sharpness of classification	Increase flow ratio	Reduce Abrasion
Cyclone diameter, D	Increase	Reduce	Increase	(-)	Increase
Inlet diameter, D_i	Increase	Reduce	-	(-)	Increase
Overflow outlet diameter, D_o	Increase	Reduce	-	Reduce	(-)
Hydrocyclone body length, L	Increase	Increase	-	Increase	(-)
Vortex finder length, l	Increase	Reduce	-	Reduce	(-)
Cone angle, θ	(-)	Reduce	Increase	(-)	(-)
Underflow diameter, D_u	(-)	(-)	(-)	Increase	(-)

As seen from the study done by Cilliers *et al*. (2004) and from the design parameter Table VI the operation of a hydrocyclone is connected to parameters and changing one parameter may have an effect to other parameters.

4.1.2 Operating parameters of hydrocyclone

The operation efficiency and properties of the hydrocyclone can be represented with multiple parameters, which are according to Svarovsky (1981; 1984): total efficiency, reduced total efficiency, overall penetration, partial efficiency, grade efficiency and cut size.

Total efficiency is the simplest way to express the efficiency of the hydrocyclone. It is defined as the ratio of solids in underflow to the total solid mass fed to the hydrocyclone. As the total efficiency represents the total mass of solids separated it does not tell the separation efficiency for certain particle sizes. Total efficiency is calculated as in equations (4.1) and (4.2).

$$E_T = \frac{M_u}{M} \qquad (4.1)$$

$$E_T = 1 - \frac{M_o}{M} \qquad (4.2)$$

Where E_T is total efficiency, M_o is the recovered mass of solids overflow, M_u is recovered mass of solids in underflow, M is the mass of solids in the feed.

Total efficiency can also be calculated from the particle size distribution from the leaving flows. The equation for calculating the total efficiency with particle size is represented in equation (4.3).

$$E_T = \frac{F_x - F_{o,x}}{F_{u,x} - F_{o,x}} \qquad (4.3)$$

Where E_T is total efficiency, F_x is percentual fraction of particle sized x in feed, $F_{u,x}$ is percentual fraction of particles having size x in underflow and $F_{o,x}$ is the percentual fraction of particles having size x in overflow. Due to the errors in measurements of particle size the determination of total efficiency in this method is not recommended.

Even the total efficiency is easy to calculate with equations (4.1) and (4.2), Svarovsky (1984) has found this as unsuitable way to express the actual separation efficiency of the hydrocyclone, because in most cases the separation efficiency depends on the size distribution and/or other features of the solids.

Reduced total efficiency takes into account the effect of dead flux or short circuiting of the flow inside the hydrocyclone. Because of this, reduced total efficiency gives always some sort of separation efficiency even if no actual solid-liquid separation would take place. This ability is the result of the fact that hydrocyclone works as a flow divider which divides solids in the flows in same ratio as the underflow divided by total feed. Underflow to feed ratio is calculated with equation (4.4) and reduced total efficiency with equation (4.5) (Heiskanen, 1987; Svarovsky 1984).

$$R_f = \frac{U}{Q} \qquad (4.4)$$

$$E'_T = \frac{E_T - R_f}{1 - R_f} \qquad (4.5)$$

Where R_f is the ratio of flow rates, U is the flow rate in underflow and Q is the underflow of the feed and E_T is total efficiency

Overall penetration tells the fraction of flow going to overflow from the total feed and is used when the small fractions are the point of interest. Overall penetration is calculated with equation (4.6).

$$P_T = 1 - E_T \tag{4.6}$$

Where P_T is overall penetration and E_T is total efficiency.

Grade efficiency is the parameter which considers only a single particle size and tells the separation efficiency for this particle. The grade efficiency does not take any other properties of the particles or other parameters of the hydrocyclone into account, which in reality have an effect on actual separation efficiency. Grade efficiency has the nature of probability as it implies to the chance for a particle to get carried out in underflow. In this case the grade efficiency is represented in so-called Tromp-curve diagram. Grade efficiency G(x) can be calculated with equations (4.7), (4.8) and (4.9) and (4.10) depending on the case at hand. Equations (4.9) and (4.10) are used when solving the grade efficiency from the under and overflows.

$$G(x) = E_T \cdot \frac{dF_{u,x}}{dF_x} \tag{4.7}$$

$$G(x) = 1 - (1 - E_T) \cdot \frac{dF_{u,x}}{dF_x} \tag{4.8}$$

$$\frac{1}{G(x)} = 1 + (\frac{1}{E_T} - 1) \cdot \frac{dF_{o,x}}{dF_{u,x}} \tag{4.9}$$

$$G(x) = \frac{M_{u,x}}{M_x} \tag{4.10}$$

Where G(x) is the grade efficiency for particle size x, E_T is the total efficiency of hydrocyclone, F_x is the cumulative percentage particles size x in the feed, $F_{u,x}$ is cumulative percentage of particles having size x in underflow and $F_{o,x}$ is cumulative percentage of particles sized x in overflow, $M_{u,x}$ is the mass flow rate of particle

sized x in underflow and M_x is the mass of particles sized x in the feed (Heiskanen, 1987; Svarovsky 1981, Svarovsky, 1984).

When calculating the realistic grade efficiency of the hydrocyclone it is important to take the dead flux into account. Corrected grade efficiency G´(x) is calculated as in equation (4.11).

$$G'(x) = \frac{G(x) - R_f}{1 - R_f} \qquad (4.11)$$

Where G(x) is the reduced grade efficiency and R_f is the ratio of overflow and underflow. The equation gives an S-shaped curve for both G(x) and G'(x) values, where the y-axis represents the probability of a particle to be carried in underflow and on the x-axis is the particle size.

4.1.3 Points in grade efficiency curve

There are some important points containing information about the operation of hydrocyclone that can be read from the grade efficiency curve. According to Svarovsky (1981) points that can be read from the curve are cut size, limit of separation and sharpness of cut.

Cut size is defined from the particle size in either of the exiting flows. The particle which has a 50% chance of been caught in to underflow or overflow. This size of the particle is considered as the equipropable particle size which is marked as x_{50}.. The cut size is at the point where curves of G(x) and G'(x) cross the line marking at 50%.

Sharpness of cut is used when the methods and equipment of solid-liquid separation is used for solids classification. It can be kept as the slope of the grade efficiency curve and defined from the slope of the tangent at the point of x_{50} or it can be represented as ratio of two particle sizes corresponding to their percentual part. For example the ratio could be represented from the masses particles having particle size x_{30} and x_{70}.

Limit of separation tells the point, where the grade efficiency of G(x) or G'(x) reaches 100%.This particle size is referred as x_{max}. Particles having this particle size are considered as the largest particles that can be found from the overflow.

4.1.4 Dimensionless quantities

Multiple variables have been identified to be fundamental for the mathematical investigation of the hydrocyclone operation. Dimensionless quantities which have been identified are Reynolds number (Re), Stokes number (Stk), Euler's number (Eu) and product between Euler's and Stokes numbers for particle size x_{50} ($Stk_{50}Eu$) (Medronho and Coelho, 2001;Svarovsky, 1981; Svarovsky, 1984).

Reynolds number is a dimensionless quantity which is used to investigate the nature of the stream. Reynolds number can be defined with two equations (4.14) and (4.15). Depending on the value of Reynolds number the current is defined as laminar, turbulent or being in transition state.

$$\mathrm{Re} = \frac{v D \rho}{\mu} \tag{4.14}$$

$$\mathrm{Re} = \frac{4Q\rho}{\pi D \mu} \tag{4.15}$$

Where Re is the Reynolds number, ν is the mean velocity, D is diameter, ρ is the density of the fluid, μ is the viscosity of the fluid and Q is the flow rate of the feed.

Euler's number is the dimensionless quantity which relates to the pressure drop Δp between the inlet and outlet of the hydrocyclone. There are two equations (4.16) and (4.17) for mathematical determination for Euler's number.

$$\mathrm{Eu} = \frac{\Delta p}{\frac{\rho v^2}{2}} \tag{4.16}$$

$$\mathrm{Eu} = \frac{\pi^2 \Delta p D_c^4}{8 \rho Q^2} \tag{4.17}$$

Where Δp is the pressure-drop, ρ is the density of the fluid and v is the fluid velocity, D_c is hydrocyclone diameter.

Stokes number relates to the behavior and movement of the particle inside the feed suspension. It is the function of the relaxation time, inner diameter of the

hydrocyclone and the velocity of the feed. Stokes number is calculated with equation (4.18).

$$Stk = \frac{\tau v}{D} \qquad (4.18)$$

Where τ is the residence time, v is the velocity of the fluid and D is the diameter of the cyclone.

The product of $Stk_{50}Eu$ is important parameter for scaling up of the hydrocyclones, as the parameter is considered to be constant as long as the geometry of hydrocyclones remains similar. $Stk_{50}Eu$ can be calculated as in equation (4.19).

$$Stk_{50}Eu = \frac{\pi(\rho_s - \rho)\Delta p D_c (x'_{50})^2}{36\mu\rho Q} \qquad (4.19)$$

Where ρ_s is the density of solids, ρ is density of fluid, Δp is pressure drop, D_c is the diameter of the cyclone, x'_{50} is the reduced cut size which is taken from the corrected grade efficiency curve, $Stk_{50}Eu$ is the product of Stokes and Euler's numbers (Medronho and Coelho, 2001).

4.1.5 Separation theories of the hydrocyclone

The theories for the separation process inside hydrocyclone can be divided according to Svarovsky (1984) into four basic theory groups: the equilibrium theory, the residence time theory, turbulent two-phase flow theory and the crowding theory. Most important ones for hydrocyclone calculations are equilibrium and residence time theory, since both are used for the calculations for the operation and design of the hydrocyclone (Svarovsky, 1984).

The equilibrium theory investigates the behavior of a particle in orbit where the tangential (some use outward terminal settling velocity) velocity and drag force pulling them to the core of hydrocyclone (inward radial velocity of the fluid) are in equilibrium, in other words when the terminal settling velocity is equal to the radial velocity of liquid. This leads to the fact that each particle settles on specific radius of orbit depending on their particle size. Large particles are assumed to attain radial orbit close the cyclone wall and small particles are carried to the middle of the hydrocyclone leading to separation in which large particles are carried downwards

to underflow and small particles are carried out with the overflow (Svarovsky, 1981, Medronho and Coelho, 2001).

These settling differences lead to the formation of locus of zero vertical velocity line (LZVV). The cut size for the hydrocyclone can be defined from the LZVV line, as the LZVV is considered as the radius of orbit for particle having particle size of x_{50}, which means that particle of this size has equal change to get carried into under- and overflows. Particles larger than x_{50} are more likely to get into underflow and the smaller are more likely to get carried into overflow. The formation of LZVV line and the vertical velocity distribution is represented in Figure 7 (Svarovsky, 1981).

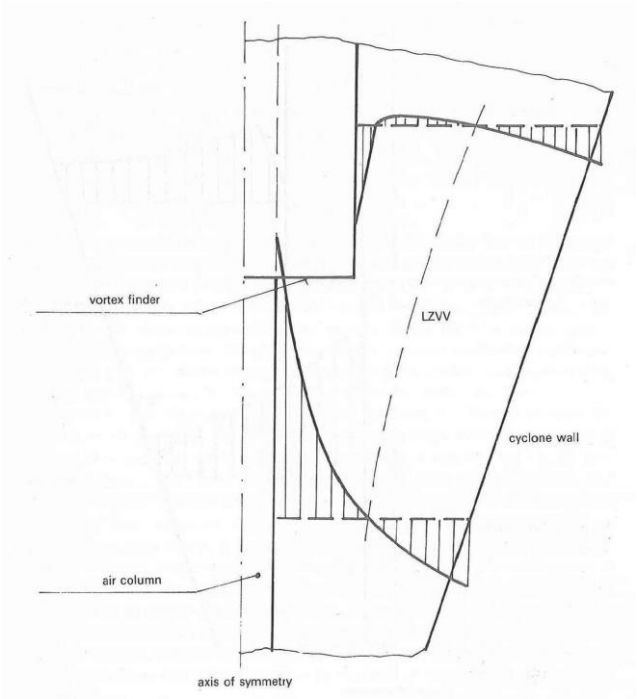

Figure 7 The formation of LZVV line to the boundary region of vertical velocity (Svarovsky 1984).

As shown in the Figure (7) the LZVV line settles in the boundary region where the vertical velocity reaches the equilibrium with the tangential velocity (Svarovsky, 1981).

Residence time theory is a theory where the conditions inside the hydrocyclone are considered to be in non-equilibrium. The theory considers the event of particle moving towards the hydrocyclone wall and is it able to reach the cyclone wall in the available residence time if it is injection place is in the middle of the inlet. The particle which is able to reach the wall in the given residence time is considered to

be the size of x_{50}. The residence time T can be expressed according to Svarovsky (1984) with equations (4.20) and (4.21)

$$\int_0^T u_r \cdot dt = \frac{1}{2} D_i \qquad (4.20)$$

$$u_r = \frac{x_{50}^2 \cdot \Delta\rho}{18\mu} \cdot \frac{v_t^2}{r} \qquad (4.21)$$

Where T is the residence time, u_r is the radial velocity of the particle and D_i is the diameter of the inlet.

4.1.6 Cut size prediction

One of the most important factors of the efficiency of a hydrocyclone is cut size as it determines the particles that are separated to under and overflows. Svarovsky (1981) suggests that the cut size is function of cyclone diameter, viscosity, density, density difference between solids and liquids and flow rate as represented in equation (4.22).

$$x_{50} = f(D_c, \mu, \rho, \Delta\rho, Q) \qquad (4.22)$$

In addition to the dependencies of the operation parameters shown above, many authors like Tavares *et al*. (2002), Coelho and Medronho (2001), and Nageswararao *et al*. (2004) have shown that the hydrocyclone design has great impact in the cut size prediction. The combination of the hydrocyclone specific variables and operation parameters lead to the fact that it is hard to form a universal model for hydrocyclone operation.

As said, the prediction of the cut size can be defined graphically from the grade efficiency curve or it can be predicted with mathematical evaluation. When the cut size is determined mathematically many of the design dependent variables need to be taken into account. Many authors have studied and developed case based models for hydrocyclones, Tavares *et al.* (2002), Coelho and Medronho (2001) and Nageswararao *et al.* (2004) for example. Coelho and Medronho (2001) studied and created a mathematical model in their study for three hydrocyclones of different design. The main properties and geometrical proportions are shown in Tables VIII.

Table VIII Size of the hydrocyclones and underflow orifice used (Coelho and Medronho, 2001)

Hydrocyclone	D_c [mm]	D_u [mm]
Rietema 1	22	2,0/4,6/6,0
Rietema 2	44	4,0/8,2/11,5
Rietema 3	88	8,5/16,0/24,7
Bradley 1	15	1,0/1,5/2,0
Bradley 2	30	2,0/3,0/4,0
Bradley 3	60	4,0/6,0/8,0
Demco 4	122	4,5/6,0/11,0/19,0

In Table IX are the geometrical proportions of the hydrocyclone that Coelho and Medronho (2001) used in their tests.

Table IX Geometrical proportions in used hydrocyclones (after Coelho and Medronho, 2001)

Geometric Ratio					
D_i/D_c	D_o/D_c	D_u/D_c	l/D_c	L/D_c	Theta [^{0}]
Range	0,14-0,28	0,20-0,34	0,04-0,28	0,33-0,55	9,0-20,0

From the data gained from the test series Coelho and Medronho (2001) derived set of equations for the operation of the hydrocyclones. Especially the prediction of cut size based on the model created seemed to be rather accurate when comparing the predicted and experimental cut size, as the actual cut size differed from the predicted cut size only a little.

The models and equations which are based on the empirical data are complex, but there are simplified models for the prediction of the cut size. Some simplified models for cut size prediction are represented in equations (4.23), (4.24) and (4.25) (Svarovsky, 1981; Wills', 2007).

$$\frac{x_{50}}{D_c} = 5{,}254 \cdot 10^{-2} \left(\frac{1}{Re_i \left(\frac{\Delta\rho}{\rho} \right)} \right)^{0,5} \qquad (4.23)$$

$$\frac{x_{50}}{D_c} = 22{,}83 \cdot 10^{-3} \left(\frac{\mu D_c}{Q \Delta\rho} \right) \qquad (4.25)$$

$$x_{50} = k\left[\frac{D_c^3 \eta}{Q_f (\rho_s - \rho)}\right]^n \qquad (4.26)$$

4.1.7 Systems of hydrocyclones

A normal way to increase the classification and separation efficiency is to put them in series. In this case the hydrocyclones can be set to run on different operating characteristics to maximize the effectiveness of the process. In addition to the series connection the hydrocyclones can work as pre-treatment for example to filtration process (Svarovsky, 1984).

Easiest way to increase the efficiency is to put hydrocyclones in simple series. In this case the total grade efficiency of the system is the combination of its parts. In Figure 8 is shown a pair of hydrocyclones with a simple connection working in a clarification process to remove fine particles from the feed.

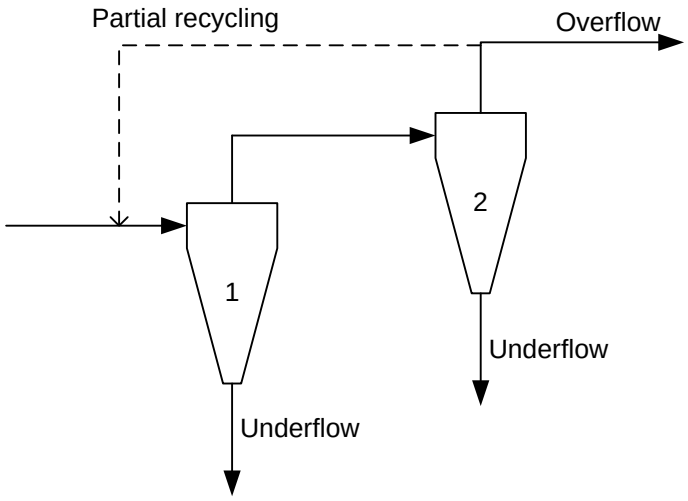

Figure 8 Hydrocyclones in series in the purpose of feed clarification (after Svarovsky, 1984).

The total grade efficiency for this kind of system is represented in equations (4.28) and (4.29). Equation (4.29) is used when there are N amount of cyclones with similar grade efficiency in the system. The partial recycling in the system could be used to improve the process.

$$G(x) = G_1 + G_2 - G_1 \cdot G_2 \qquad (4.28)$$

$$G(x) = 1 - (1 - G_1)^N \qquad (4.29)$$

Where $G_{(x)}$ is the grade efficiency for whole system, G_1 and G_2 are the grade efficiencies of cyclone 1 and 2 respectively and N is the number of cyclone in series. As seen from the Figure 8 it would be wise to have the following hydrocyclone or -cyclones working with smaller cut size to maximize the efficiency of the clarification process (Svarovsky, 1984)

Hydrocyclones can be put in series for then the purpose of thickening. Example setting is represented in Figure 9. This set-up could be for example in use in tailings thickening facilities.

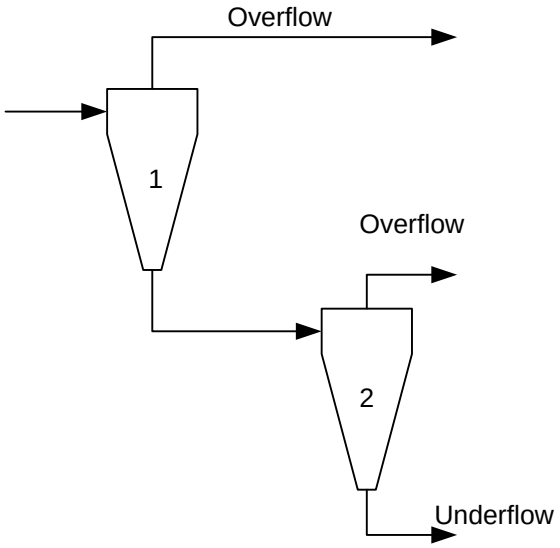

Figure 9 Hydrocyclones connected in series for the purpose of feed thickening (after Svarovsky, 1984).

When the hydrocyclones are connected as in Figure 8 the total efficiency of the system is calculated as in equation (4.30).

$$G(x) = \frac{G_1 \cdot G_2}{1 - G_1 + G_1 \cdot G_2} \qquad (4.30)$$

If the feed is dilute or the product wanted needs to be thick as possible the example set-up in Figure 10 could be used. In this case the total efficiency for the process is calculated as in equation (4.31).

$$G(x) = \frac{G_1 \cdot G_3}{1 - G_1 \cdot G_2 \cdot (1 - G_3)} \qquad (4.31)$$

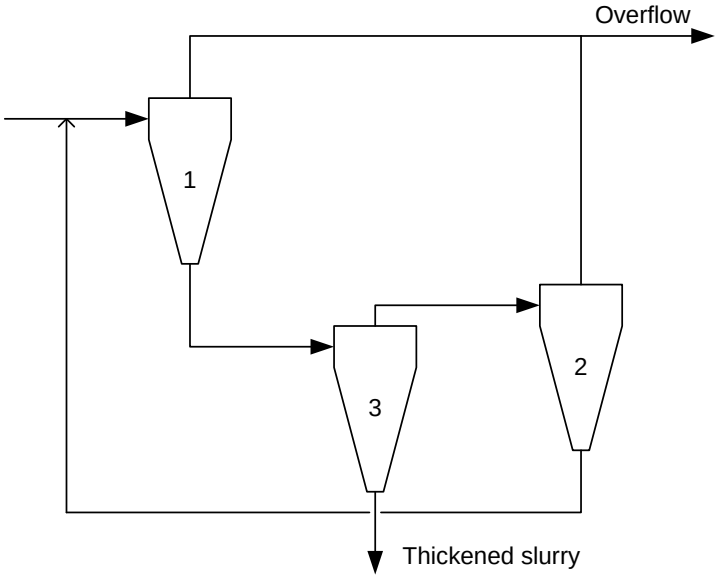

Figure 10 Thickening for dilute solids (After Svarovsky, 1984).

In this set-up, the hydrocyclone number 1 would work as a clarifier as in Figure 8 and the hydrocyclones 2 and 3 would work as thickeners number 3 being the main product maker.

The combination shown in Figure 11 could be used for creating a pre-coat layer for filter when filtering slurries.

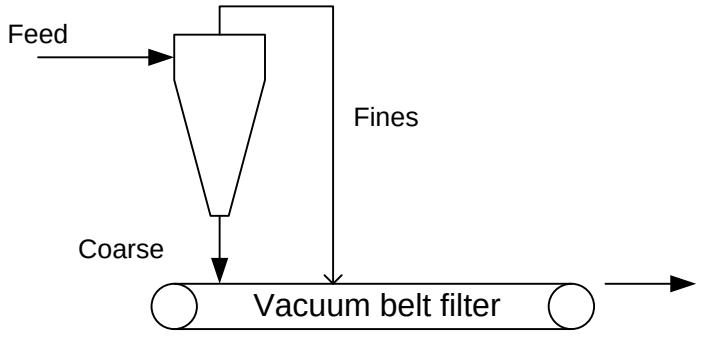

Figure 11 Hydrocyclone and belt filter (After Svarovsky, 1984).

The combination shown in Figure 17 could be used in the slime thickening operation. After hydrocyclone the sieve would separate fines still remaining in the thickened product and coarse particles. The filtrate and overflow from the hydrocyclone would be combined and lead to thickener for slime thickening.

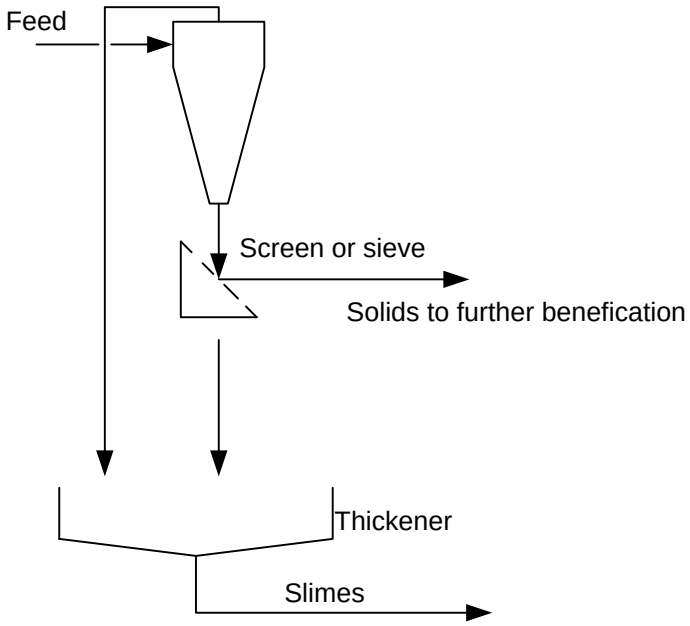

Figure 12 Slime thickening (After Svarovsky, 1984).

As seen from the few examples the hydrocyclone can be combined with other equipment and opera in multiple different roles in processes.

4.2 Thickeners

Thickeners are commonly used in industry for treatment of process waters and waste waters. The operation principle of thickeners is based on sedimentation of the particles and it is at its most effective stage when the density difference between liquid and solids is as big as possible. Different size particles have different kind of sedimentation speeds depending on their particle size, shape, density and viscosity of the liquid. The sedimentation process can be accelerated by adding flocculants to the slurries. Especially when the slurry contains very small particles of which have colloidal nature the addition of flocculants is more or less necessary to have satisfactory sedimentation. The addition of flocculants causes the particles to attach on each other forming larger particle flocks, which fasten the sedimentation speed (Wills', 2006).

Thickening process can be done in batches, or the thickening process can be continuous. Continuous thickeners are constructed from large vessel which can be over hundred meters in radius and have depth of several meters and from the rake which scoops the settled solids to the underflow outlet. The slurry is pumped to

vessel through feed inlet and the clarified overflow water is lead out through overflow launder. As the rake turns around it scoops the sedimented solids towards the middle section of the thickener where they are discharged. Simplified picture from the structure of thickener is presented in Figure 13.

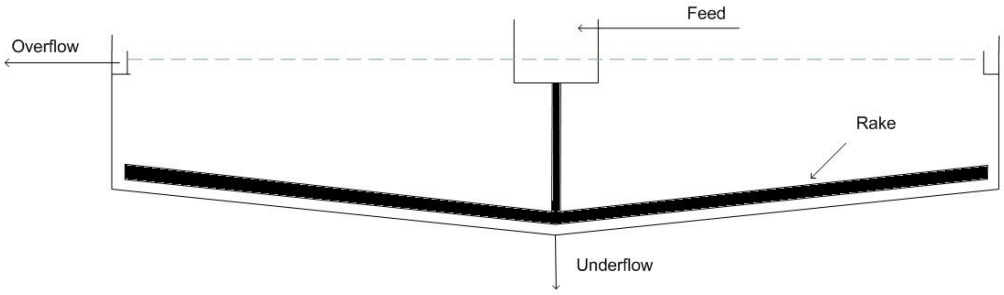

Figure 13 Simplified cross-cut figure from a thickener (after Wills, 2007).

4.3 Filtration equipment

Filters are used in dewatering processes to maximize the dry content in the tailings. Especially when the tailings are drystacked the treatment for dewatering is the filtration of the tailings slurry. The type of filter and the required driving forces are determined by the nature of the slurry, as the composition of the slurry determines the requirements for the needed filter media. The range of different kind of filters is wide, but there are couple main categories of filters: vacuum and pressure filters (Svarovsky, 1981).

Vacuum filters are operated with low driving forces which can be created by creating a under pressure behind the filter media, or letting the slurry to settle on top of the filter media by gravitational settling. Vacuum filters have the advantage of being easy to be made continuous, where pressure filters tend to have batch-like nature. Belt and rotary drum filters are good examples of the vacuum filters.

Pressure filters are used when the nature of the slurry/suspension requires high driving force, which can be created with compression. Reasons that can lead to the use of pressure filtration are for example low settling velocity of the solids inside the suspension or the particle size of the solids in the slurry. The driving force is generated either by pumping the slurry with high pressure or compressing the chamber where the slurry is pumped. Typical pressure filters are for example filter presses.

EXPERIMENTAL PART

Two different types of tailings were used in the studies. They were identified to have different sulphur concentrations (high and low) and their particle size distribution profile and solid concentration of the slurries were different. The main target of the experimental part was to investigate the effect of the changes in the geometric proportions of the hydrocyclone to fractionation of the solids by changing the over- and underflow spigots. Changes in the fractionation were determined by analyzing the particle size profiles of over- and underflows and changes in solid concentration.

Before starting the experiments preliminary tests for slurries were done to determine the following basic properties of the slurry:

1. Solid concentration
2. Density of solids
3. Density of the slurry
4. Particle size distribution

During the experiments also the flowrates of over- and underflows were measured.

5 EXPERIMENTAL PLAN, EQUIPMENT AND RESEARCH METHODS

An experimental design was made for both slurries containing total of 12 measurement points each. The basis for creating the experimental plan was to study the effectiveness of changing the configuration of underflow and overflow spigots. The different settings consisted all available combinations of over- and underflow spigots that were accompanied with the test hydrocyclone. The set consisted underflow spigots of 3 mm, 5 mm, 6 mm and 8 mm. Overflow spigots that were used consisted from 8 mm, 11 mm and 14 mm spigots. Measurement point table for different spigot configurations is represented in Table X where measurement points 1-12 are for high sulfuric tailings and points 13-24 are for low sulfuric tailings.

Table X The measurement point table for high and low sulphuric tailings.

Overflow spigot size [mm]	Underflow spigot size [mm]				
	8	6	5	3	
14	1 | 13	2 | 14	3 | 15	4 | 16	Measurement point number
11	5 | 17	6 | 18	7 | 19	8 | 20	
8	9 | 21	10 | 22	11 | 23	12 | 24	

5.1 Equipment

The equipment that were used in the tests contained a MOZLEY C124 two inch hydrocyclone, pressure air powered mixer, mono pump with pump chamber made out of acid-proof steel, 1.5 kW electric engine which ran the pump and a storage/mixing tank which was connected to the pump. Piping of the hydrocyclone was made out of iron or plastics. The layout of the setting is represented in Figure 14.

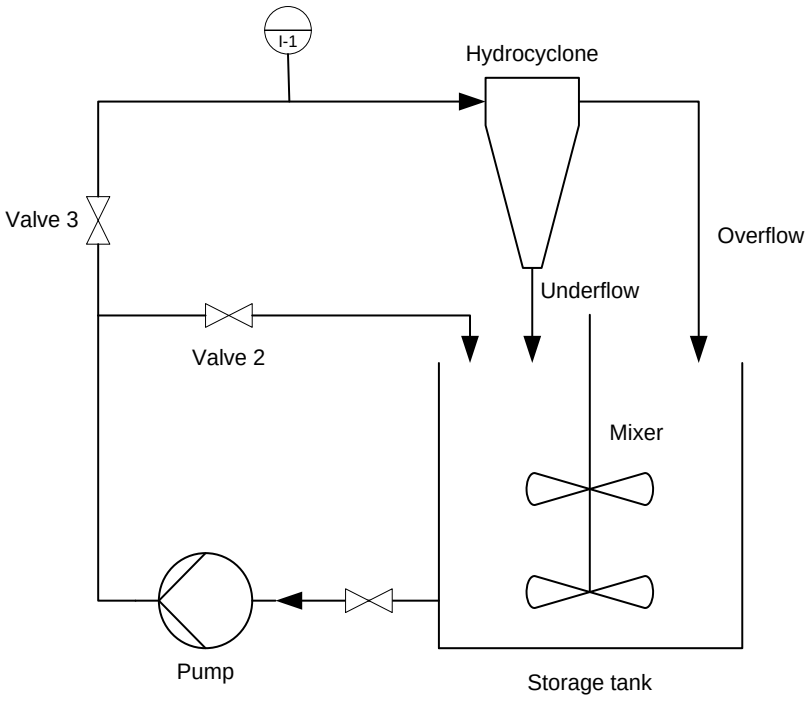

Figure 14 Layout of the test equipment.

To ensure the wanted homogenization and to prevent the sedimentation of the solids the tank was constantly mixed with the mixer and before sampling the mixing

procedure was empowered by pumping the slurry though the system for 30 minutes to let the flow settle. During the settling of the flow the pressure was adjusted to wanted pressure of 2 bars by adjusting the flow going through the hydrocyclone by adjusting valve 2 which allowed some of the slurry to bypass the main flow reducing the pressure in hydrocyclone. Test for both slurries were carried out in ambient temperature of 24 ºC, though because of the pumping some warming of the slurry could be noticed.

Samples were taken with measurement vessels with volume scale simultaneously from the over- and underflows. Three separate samples were taken at each measurement point and each time the volume and duration of the sample taking time was also recorded. Total number of samples taken for the slurries was 36 each. From over- and underflow samples smaller samples were taken aside for further studies and the remaining surplus slurry from larger sample vessels was poured to separate trash canister to prevent any changes i.e. particle size distribution and solid concentration in the mother slurry.

Particle size distributions were determined by using Malvern Mastersizer 3000 particle size analyzer. The particle size analysis was based on laser diffraction and different methods can be used for particle size determination. In this study Fraunhofer model was used.

The sample for particle size analysis was made by taking a small amount of slurry from previously taken slurry samples from under- and overflow streams. The slurry was then mixed with purified water in small beaker. The diluted sample was then added to the sample beaker (full of purified water) in the particle size analyzer as long as the required limit was achieved. Each particle size analysis included five separate runs and from the acquired data an average result was made which was then used as the basis of the analysis results. Analyzes were done with at least two different samples at corresponding measurement point for both under- and overflow slurries.

5.2 Determination of the basic properties of low and high sulfuric tailing slurries

The definition of the solid concentrations for slurries and test samples were carried out by taking a sample and weighing it which was followed by drying it in a heating chamber in 120 ˚C for at least 24 hours. After the drying the sample was weighted again and the solid concentration was calculated from the weight difference.

The density of the slurries were determined by taking a sample from the current going through Valve 2 into a vessel, and then weighed on a laboratory scale from, which volume and density was determined by the mass.

The true density of solids in the slurries was determined based in mixing some of the dried solids with distilled water. The determination of true densities of solids was carried out with following procedure:

1. Glass cylinder was put on laboratory scale and the scale is set to zero.
2. A sample of dried solids from slurry was poured into a glass cylinder so that the total volume of solids occupied 20 mL from the cylinder. The mass of the solids was measured.
3. Vessel was filled to mark of 100 mL and the suspension of was mixed well and weighted.
4. The weight fraction c_w and slurry density ρ_{sl} were calculated by with equations (5.1) and (5.2).

$$c_w = \frac{m_s}{m_{sl}} \qquad (5.1)$$

$$\rho_{sl} = \frac{m_s}{m_{sl}} \qquad (5.2)$$

5. The True density of solids was calculated with the equation (5.3)

$$\rho_s = \frac{\rho_{sl} c_w \rho_l}{\rho_l - \rho_{sl}(1 - c_w)} \qquad (5.3)$$

The flow rate of the under- and overflows were determined by taking time as two vessels with volume scale were introduced under both currents simultaneously. After a batch from both currents was taken the volume was measured and the time it took to fill was noted. The complete set of the results from flow rate measurements can be found for high sulfur slurry in Appendix I and for low sulfur slurry in Appendix II.

6 MEASERUMENT RESULTS

Before any of the samples were taken from the hydrocyclone preliminary tests were done for both tailing slurries. Parameters that were investigated were, solid concentration, slurry and solid density and particle size distribution.

6.1 Determination of the properties of high sulfur and low sulfur tailings

The density of both slurries were determined by taking a sample of constantly mixed slurry from the flow going through Valve 2 and weighing it on analytical scale. The density of the high sulfuric tailings was measured to be approximately 1079 kg m^{-3} with standard deviation of 12,68 kg m^{-3} and mean error of 4,01 kg m^{-3}. For low sulfur tailings the density of the slurry was approximately 1062 kg m^{-3} with standard deviation of 16,42 kg m^{-3} and mean error of 7,34 kg m^{-3}.

The solid content of the slurries were determined by drying three separate samples from the mixed slurries. The average solid content for high sulfur tailings was approximately 13 w-% with standard deviation of 0,57 %-units and mean error of 0,37 %-units. For low sulfuric tailings slurry the solid content was noticed to be almost 26 w-% so a diluted suspension had to be made before any tests with hydrocyclone could be done. The diluted suspension was made by pumping half of well mixed original slurry to another container and replacing the pumped amount with same amount of water resulting in suspension with solid concentration of 12,25

w-% with standard deviation of 0,81 % and mean error of 0,40 %. Results from solid content and density measurements are shown in Appendix I.

The true density of tailings solids were calculated with the procedure containing equations 5.1, 5.2 and 5.3. True density for the solids of high sulfur tailings was approximately 3155 kg m^{-3} and for the low sulphur tailings 2907 kg m^{-3}.

To get understanding of the particle size distribution for the tailings samples were taken from the stream bypassing main flow and analysed with Malvern Mastersizer 3000 particle size analyser. The results for both particle size and cumulative volumetric particle size distribution for both high and low sulphur tailings are represented in Figure 15.

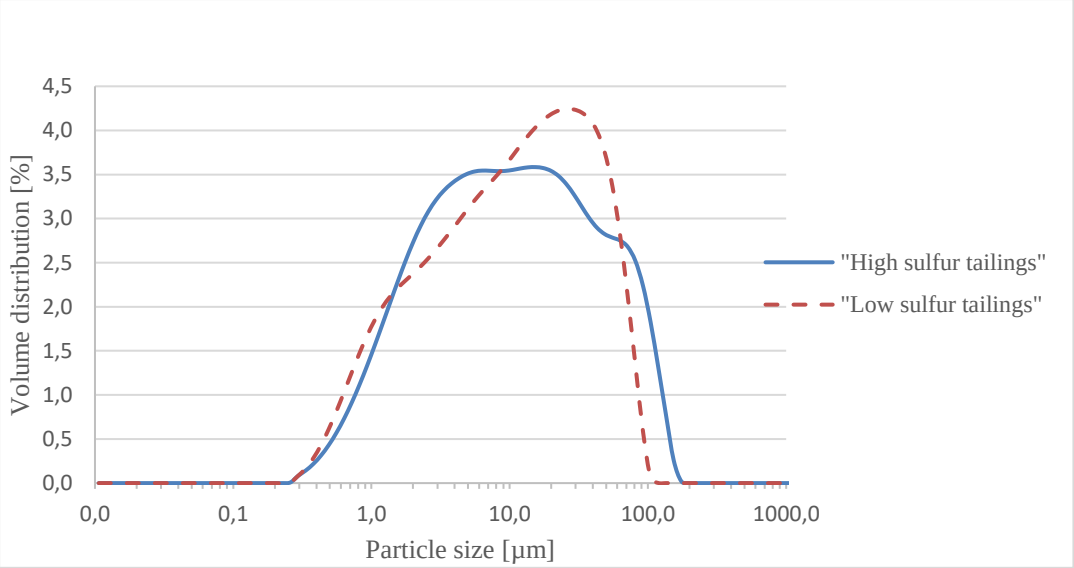

Figure 15 Volumetric particle size distribution for low and high sulfuric tailings

According to the particle size analysis the d_{10} for high sulfur tailings was 1.52 µm, d_{50} 10.1 µm and d_{90} 65.8 µm. Values for low sulfuric tailings d_{10} was 1.30 µm, d_{50} 10.9 µm and was d_{90} 48.9 µm. As from the Figure 15 can be seen that both tailings have rather broad particle size distribution.

6.2 Results of the measurement points of high sulphur slurry

High sulphur tailings were studied according to the research plan where in total of 12 measurement points were studied.

Measurement points 1-4 were carried out by using 14 mm overflow orifice. After the samples were analysed, values for d_{10}, d_{50} and d_{90} could be obtained. The overall results including solid concentration are represented in Table XII.

Table XI Collected results from particle size analysis and solids for points 1 (8mm), 2 (6 mm), 3 (5 mm), 4 (3 mm)

Overflow						
Underflow spigot size [mm]	d10 [µm]	d50 [µm]	d90 [µm]	Mean solids [w-%]	STDdev [%-units]	Mean error [%-units]
8	1,04	3,43	12,1	7,48	0,05	0,03
6	1,04	3,33	11,7	7,39	0,13	0,08
5	1,06	3,52	12,7	7,44	0,41	0,24
3	1,1	3,93	14,4	8,26	0,05	0,03
Underflow						
Underflow spigot size [mm]	d10 [µm]	d50 [µm]	d90 [µm]	Mean solids [w-%]	STDdev [%-units]	Mean error [%-units]
8	2,51	18,3	76	35,37	3,11	1,79
6	3,01	15,3	44,6	49,68	5,59	0,08
5	4,09	14,7	36,5	47,13	14,7	0,24
3	6,59	18,7	44,1	68,08	0,03	0,01

Volumetric particle size distributions of the overflow for points 1-4 are represented in Figure 16.

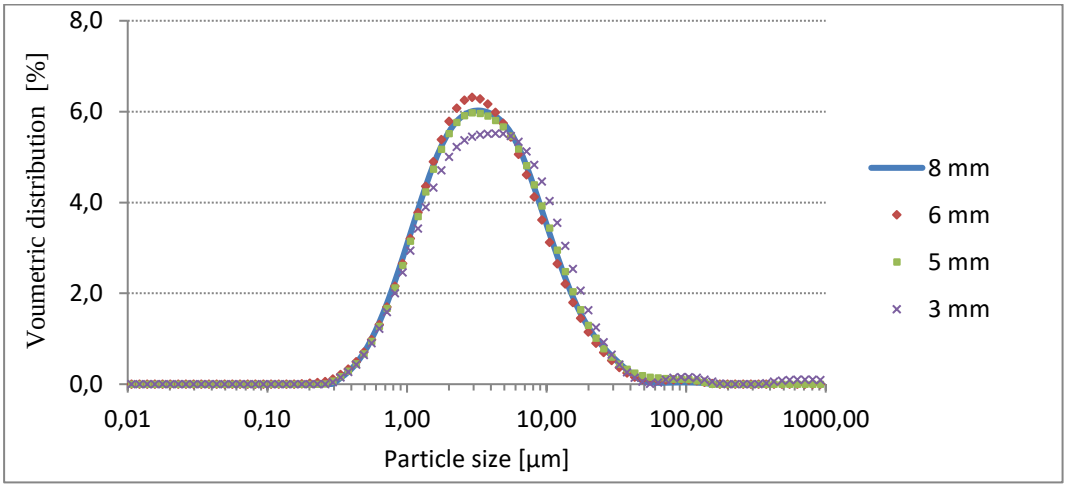

Figure 16 Volumetric particle size distribution of overflow for points 1 (8mm), 2 (6 mm), 3 (5 mm), 4 (3 mm)

As from the Figure 16 can be seen the change of the underflow spigot has very small influence on the particle size distribution in the overflow.

The volumetric particle size distributions for the underflows of points 1-4 are represented in Figure 17.

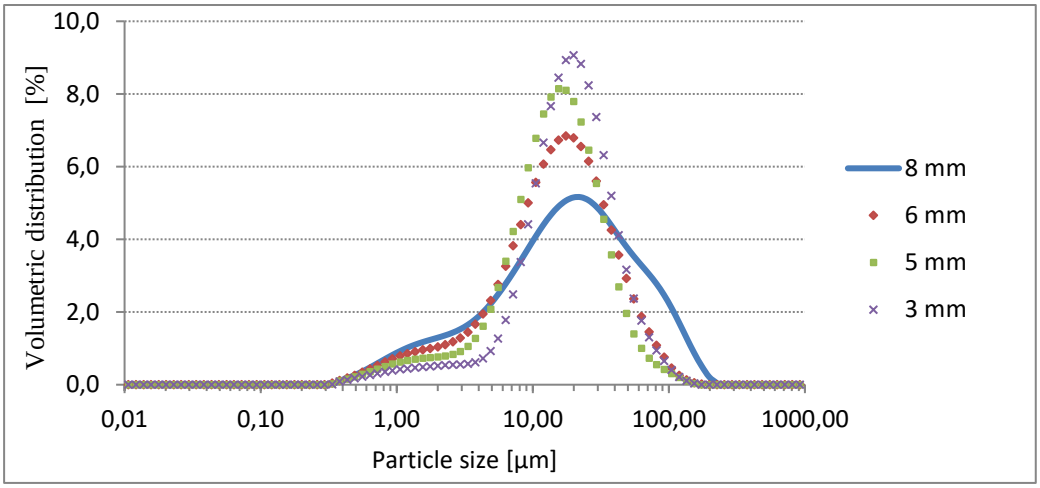

Figure 17 Volumetric particle size distribution of underflow for the measurement points 1 (8mm), 2 (6 mm), 3 (5 mm), 4 (3 mm)

As from the Figure 17 can be seen changing the size of underflow spigot has very significant effect on volumetric particle size distribution as the main fraction of particles are over 10µm in size. This change on particle size distribution can be seen also in the change in the solid concentrations in underflow samples as shown previously in Table XI.

The rather drastic change in the solid concentrations of the underflow slurries can be explained as by tightening the gap increases the requirement of kinetic energy of particles to exit hydrocyclone from the underflow gap. This means that only the heavier and particles with greater in volume have enough kinetic energy to push down in hydrocyclone and exit through underflow orifice. Particles and liquid which do not have the required energy are pushed upwards and exit through the overflow orifice.

Flowrates for each configuration was measured by taking time and obtaining a sample from both currents simultaneously. The results for over and underflow currents are shown in Table XII.

Table XII Flowrates for points 1 (8mm), 2 (6 mm), 3 (5 mm), 4 (3 mm)

Overflow				
Underflow spigot size [mm]	Mean time [s]	Mean Flow [mL/s]	STDdev [mL/s]	Mean error [mL/s]
8	4,05	649,11	25,71	11,5
6	3,49	754,03	28,4	12,7
5	1,61	727,65	70,14	40,49
3	3,7	790,06	37,37	16,71
Underflow				
Underflow spigot size [mm]	Mean time [s]	Mean Flow [mL/s]	STDdev [mL/s]	Mean error [mL/s]
8	4,05	206,39	9,39	4,2
6	3,49	93,6	3,81	1,7
5	1,61	43,44	2,99	1,73
3	3,7	21,51	1,24	0,56

Total mean flowrates were: Point 1: 855,5 mL/s, point 2: 847,62 mL/s., point 3: 771 mL/s. and point 4: 811,57 mL/s. The ratios between the over and underflows change drastically as with 8 mm underflow and 14mm overflow spigot is approximately 3:1 but when the size is reduced to 3 mm spigot the ratio is 40:1

6.2.1 Measurements with 11 mm overflow orifice

Measurement points 5-8 were done by using 11 mm overflow orifice. Pumping pressure and other parameters were kept as same as with previous four measurement points. After the samples were analysed, values for d_{10}, d_{50} and d_{90} could be obtained. The overall results including solid concentration are represented in XIII a and XIII b.

Table XIII a Collected results from particle size analysis and solids for points 5 (8 mm), 6 (6 mm), 7 (5 mm) and 8 (3 mm)

Overflow						
Underflow spigot size [mm]	d_{10} [µm]	d_{50} [µm]	d_{90} [µm]	Mean solids [w-%]	STDdev [%-units]	Mean error [%-units]
8	0,95	2,68	8,45	5,97	0,12	0,082
6	0,96	2,75	8,53	6,12	0,14	0,08
5	0,95	2,89	9,37	6,46	0,12	0,07
3	1,02	3,27	10,8	7,35	0,06	0,04

Table XIII b Collected results from particle size analysis and solids for points 5 (8 mm), 6 (6 mm), 7 (5 mm) and 8 (3 mm)

Underflow						
Underflow spigot size [mm]	d_{10} [µm]	d_{50} [µm]	d_{90} [µm]	Mean solids [w-%]	STDdev [%-units]	Mean error [%-units]
8	1,62	10,4	41	22,97	2,62	0,85
6	1,84	11,1	35,7	29,92	0,42	0,24
5	2,43	12,4	34,8	43,03	2,17	1,25
3	5,23	15,8	38,5	65,86	0,9	0,52

From the particle analyses can be seen that when the size of the overflow orifice was reduced the d-values for both over and underflow reduced compared to the 14 mm orifice results. Also the solid concentrations reduced in underflow when using spigots of size 8 mm and 6 mm. As with the 14 mm orifice the change of spigot has quite small effect on the solid concentration in the overflow.

The volumetric particle size distributions of overflows for points 5-8 are represented in Figure 18.

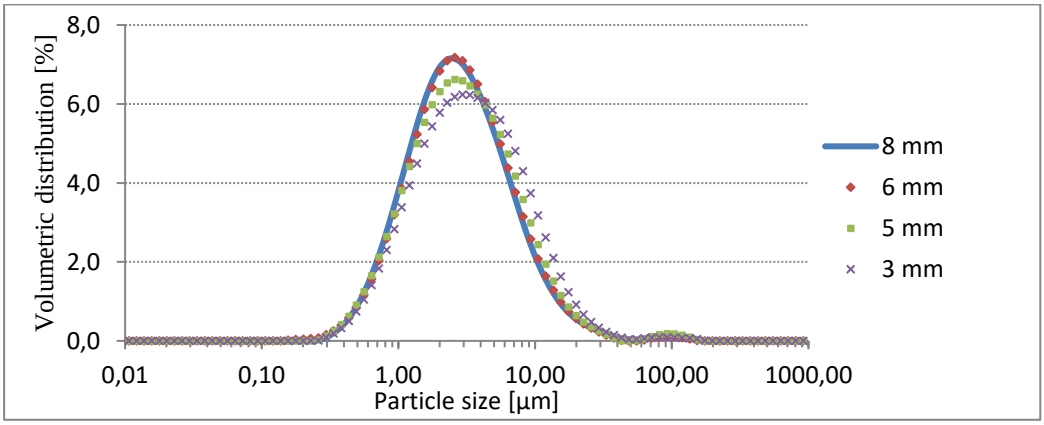

Figure 18 Volumetric particle size distribution of overflow for points 5 (8 mm), 6 (6 mm), 7 (5 mm) and 8 (3 mm)

In Figure 18 can be seen some effect of the change of the spigot size, as the 3 mm spigot shows some shifting of the distribution curve towards bigger particles. Otherwise the overflow curve of 11 mm orifice resembles same behaviour as previous with the 14 mm orifice.

Volumetric particle size distributions for the underflows of points 5-8 are represented in Figure 19.

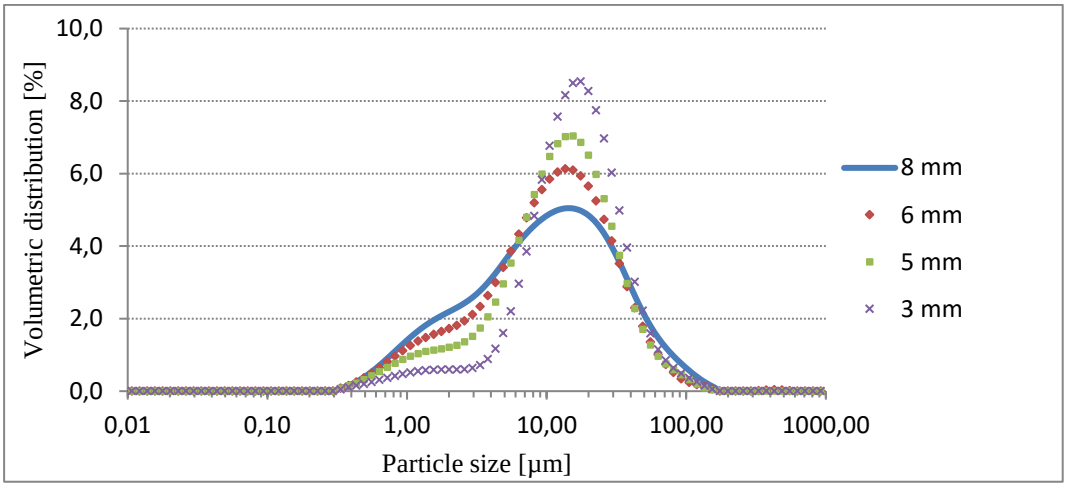

Figure 19 Volumetric particle size distribution of underflow for points 5 (8 mm), 6 (6 mm), 7 (5 mm) and 8 (3 mm)

Same effect of the spigot change can be seen from the Figure 19 which happened with 14 mm orifice tests. As the orifice size reduces more and bigger particles are carried into the underflow and by doing this they push water and lighter particles to overflow. Especially the 3 mm and 5 mm spigots seem to distinguish particles under 4 µm out of the current.

The measured flowrates for points 5-8 are represented in Table XIV

Table XIV Flowrates for measurement points 5 (8 mm), 6 (6 mm), 7 (5 mm) and 8 (3 mm)

Overflow				
Underflow spigot size [mm]	Mean time [s]	Mean Flow [mL/s]	STDdev [mL/s]	Mean error [mL/s]
8	5,36	409,93	9,4	4,21
6	4,78	504,72	30,37	13,58
5	2,3	552,52	17,08	7,64
3	5,15	612,65	24,35	10,89
Underflow				
Underflow spigot size [mm]	Mean time [s]	Mean Flow [mL/s]	STDdev [mL/s]	Mean error [mL/s]
8	5,36	298,61	5,84	2,61
6	4,78	144,78	6,44	2,88
5	2,3	72,05	3,79	1,69
3	5,15	26,41	1,15	0,51

Total mean flowrates were: Point 5: 708,54 mL/s, point 6: 649,49 mL/s , point 7: 624,57 mL/s and point 8: 639,06 mL/s. Compared with the previous 4 the ratios between over and underflows are rather different. This is explained with the change

of ratio between orifice and spigot. For example the ratio of under/overflow with 8 mm spigot is 3:4 as with 14 mm orifice the ratio was 1:3.

6.2.2 Measurements with 8 mm overflow orifice

Points number 9-12 were carried with 8 mm overflow orifice. After the samples were analysed, values for d_{10}, d_{50} and d_{90} could be obtained. The overall results including solid concentration are represented in XV.

Table XV Collected results from particle size analysis and solids from points 9 (8 mm), 10 (6 mm), 11 (6 mm) and 12 (3 mm)

Overflow						
Underflow spigot size [mm]	d10 [µm]	d50 [µm]	d90 [µm]	Mean solids [w-%]	STDdev [w-%]	Mean error [w-%]
8	0,897	2,34	9,97	4,61	0,02	0,01
6	0,906	2,41	7,57	5,07	0,05	0,03
5	0,961	2,7	8,03	5,87	0,16	0,09
3	0,961	2,7	8,03	5,87	0,16	0,09
Underflow						
Underflow spigot size [mm]	d10 [µm]	d50 [µm]	d90 [µm]	Mean solids [w-%]	STDdev [w-%]	Mean error [w-%]
8	1,2	5,28	20,6	11,96	0,03	0,02
6	1,26	6,1	20,5	14,77	0,02	0,01
5	1,49	7,46	21,7	19,6	0,1	0,05
3	2,61	10,9	30,1	42,66	0,84	0,48

From the particle size analyses can be seen same reduction on the d- values. Also it is notable that the solid concentration in both over and underflow are reduced greatly. From the 11 mm orifice the solid concentration has reduced to approximately half same progress can be seen with overflow solid concentration. The volumetric particle size distributions for overflows of points 9-12 are represented in Figure 20.

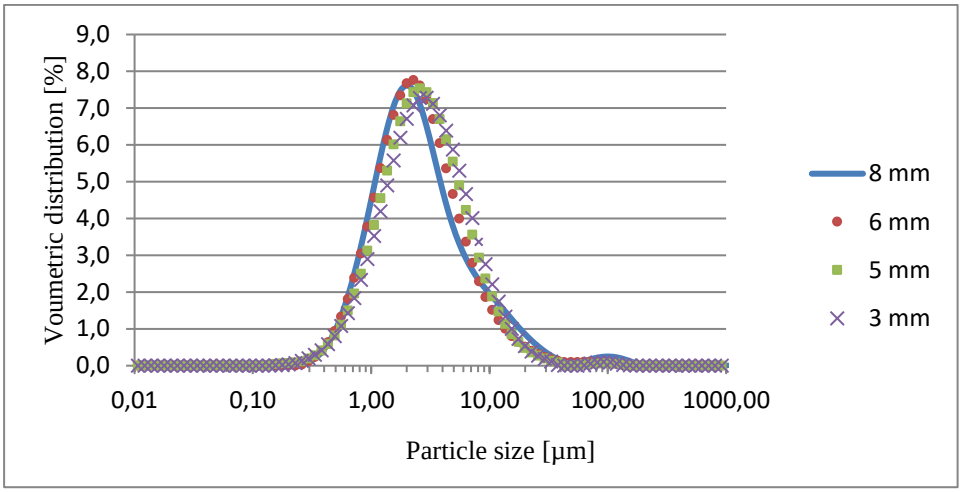

Figure 20 Volumetric particle size distribution of overflow for points 9 (8 mm), 10 (6 mm), 11 (6 mm) and 12 (3 mm)

From the volumetric particle size distribution can be seen same phenomena as with 11 mm orifices: spigots of 5 mm and 3 mm spigots increase the amount of larger particles in the overflow. The small peak at the particle size of 100 µm might be a measurement error or contamination of the sample, which could be rust particles which have been detached from the surfaces of the piping.

Volumetric particle size distributions for underflow of points 9-12 are represented in Figure 21.

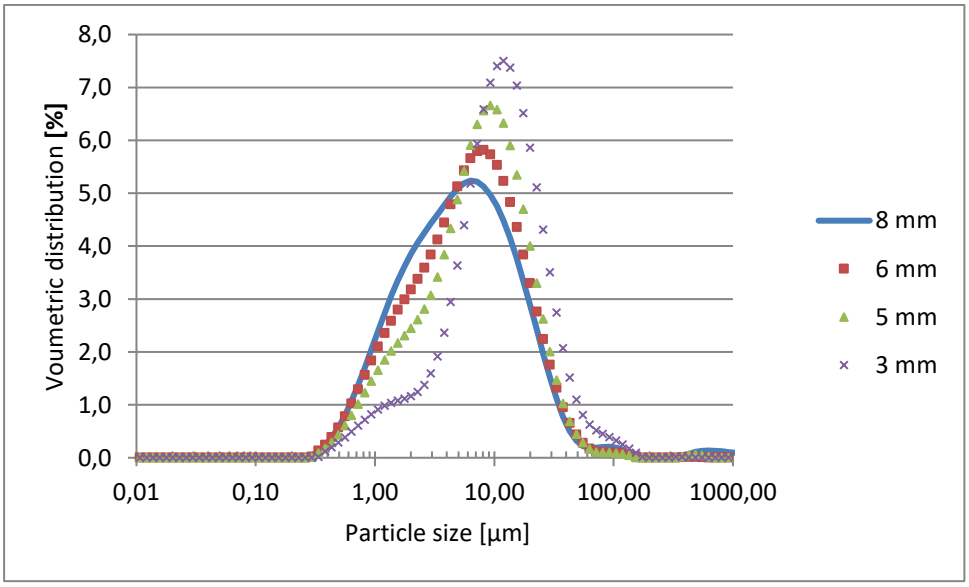

Figure 21 Volumetric particle size distribution of underflow for point**s 9** (8 mm), 10 (6 mm), 11 (6 mm) and 12 (3 mm)

The distribution curves at Figure 21 follow the trend that has been with other underflow measurements. Although there is major leap in the curve at 3 µm, which

could indicate that with this configuration the separation of particles smaller than 3 µm is very effective.

Flowrates for points 9-12 are represented in Table XVI.

Table XVI Flowrates for points 9 (8 mm), 10 (6 mm), 11 (5 mm) and 12 (3 mm)

Overflow				
Underflow spigot size [mm]	Mean time [s]	Mean Flow [mL/s]	STDdev [mL/s]	Mean error [mL/s]
8	5,17	194,96	9,44	4,22
6	7,11	274,74	6,36	2,6
5	3,93	531,26	159,33	65,05
3	3,48	386,3	131,08	58,62
Underflow				
Underflow spigot size [mm]	Mean time [s]	Mean Flow [mL/s]	STDdev [mL/s]	Mean error [mL/s]
8	5,17	363,13	62,31	27,87
6	7,11	223	29,05	11,86
5	3,93	116,52	4,34	1,77
3	3,48	39,18	1,74	0,78

Flowrate results from 8 mm orifice distinguish quite well from the previous ones, as the overflow current is smaller than underflow current. But when the spigot size is reduced the overflow current gets bigger. At the point of spigot size of 3 mm it is clear that the hydrocyclone is choked as the total flowrate compared to others drops significantly. Total flowrates are: Point 9: 558,09 mL/s, point 10: 497,74 mL/s, point 11: 647,78 mL/s and point 12: 425,48 mL/s.

6.3 Results of low sulphuric tailings slurry

High sulphur tailings were studied according to the research design where in total of 12 measurement points were studied. The points that included in the analyses of low sulphur slurry are 13-24.

6.3.1 Measurement with 14 mm overflow orifice

The measurement points 13-16 were carried out with the overflow orifice diameter of 14 mm. After the particle size analysis from the particle size analyser values for

d_{10}, d_{50} and d_{90} could be obtained. The collected results including solid concentration are represented in Table XVII.

Table XVII Collected results from the particle size and solid concentration analysis for measurement points 13 (8 mm), 14 (6 mm), 15 (5 mm) and 16 (3 mm)

Overflow						
Underflow spigot size [mm]	d10 [µm]	d50 [µm]	d90 [µm]	Mean solids [%]	STDdev [w-%]	Mean error [%-units]
8	0,898	3,07	11,1	3,79	0,08	0,05
6	0,898	3,07	11,1	3,79	0,08	0,05
5	0,909	3,2	10,9	4,32	0,07	0,04
3	1,06	5,99	26,5	7,91	0,2	0,11
Underflow						
Underflow spigot size [mm]	d10 [µm]	d50 [µm]	d90 [µm]	Mean solids [%]	STDdev [w-%]	Mean error [%-units]
8	2,68	20,4	69,2	32,67	0,23	0,13
6	5,79	30,6	102	52,4	1,88	0,01
5	9,35	40,1	126	72,36	0,65	0,04
3	23,8	73,6	178	73,73	1,2	0,11

The volumetric particle size distribution for the overflow of points 13-16 are represented in Figure 22.

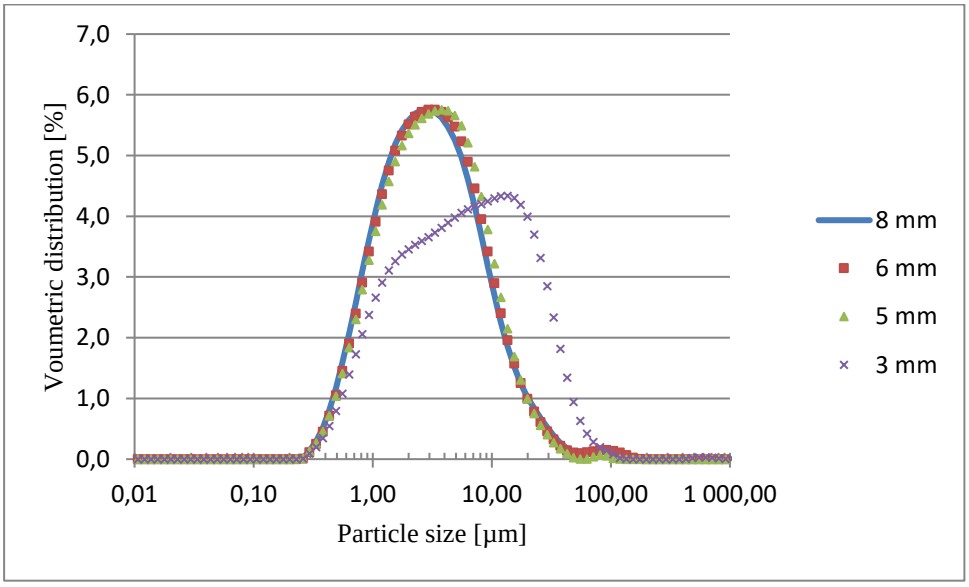

Figure 22 Volumetric particle size distribution from overflow of points 13 (8 mm), 14 (6 mm), 15 (5 mm) and 16 (3 mm)

The distribution curve of 3 mm spigot distinguishes well from others as well as in the results from the curve from the high sulphur content (Figure 17). Otherwise the

curves of 8 mm, 6mm, and 5 mm spigots follow the same trend together with high sulphur samples.

From the results can be seen as from the previous ones that decreasing the size of the underflow gap has very little effect on the particle size distribution of the Overflow, except for 3 mm spigot. Volumetric particle size distribution of underflow for points 13-16 can be seen from Figure 23.

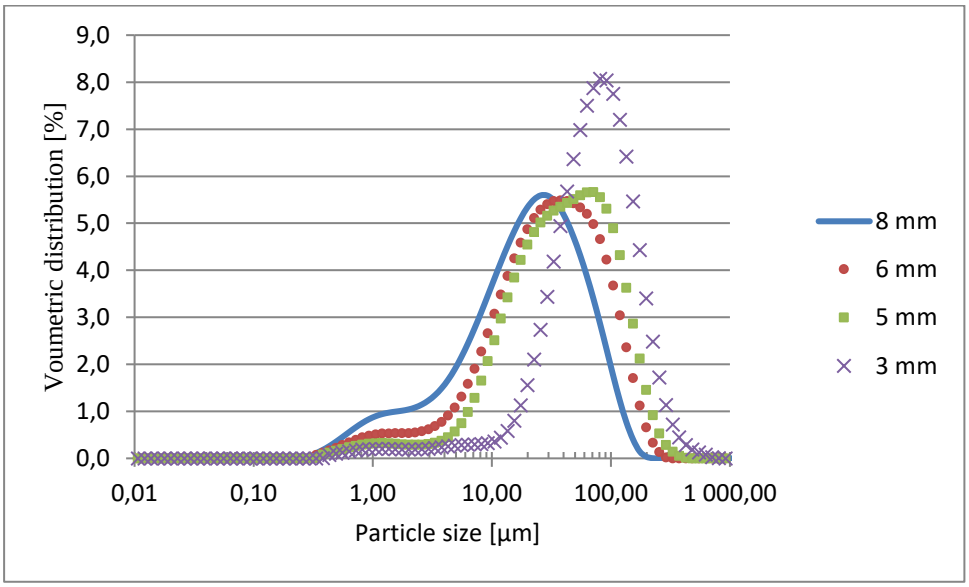

Figure 23 Volumetric particle size distribution for the underflow of measurement points 13 (8 mm), 14 (6 mm), 15 (5 mm) and 16 (3 mm)

In the Figure 33 the curve of 3 mm spigot pops out clearly. When studying the cumulative particle size distribution figure which is shown in Figure 34 the behaviour of the overflow curves might be explained. It seems that this configuration favours big particles (d_{50} is 73 µm) resulting to the fact that smaller particles have to end up into overflow, which would explain the behaviour at the overflow current.

Flowrates from measurement points 13-16 are represented in Table XVIII

Table XVIII Flowrates of points 13 (8 mm), 14 (6 mm), 15 (5 mm) and 16 (3 mm)

Overflow				
Underflow spigot size [mm]	Mean time	Mean Flow [mL/S]	STDdev [mL/s]	Mean error [mL/s]
8	4,73	603,64	17,91	8,96
6	2,19	752,35	7,61	3,40
5	1,99	734,11	61,02	35,23
3	1,67	891,28	64,64	28,91
Underflow				
Underflow spigot size [mm]	Mean time	Mean Flow UF [mL/s]	STDdev [mL/s]	Mean error [mL/s]
8	4,73	208,63	2,68	1,34
6	2,19	131,60	5,38	2,40
5	1,99	79,92	5,63	3,25
3	1,67	81,23	5,83	2,61

Total flowrates: Point 13: 812,27 mL/s, point 14: 881,95 mL/s, point 15: 814,03 mL/s point 16: 972,51 mL/s.

6.3.2 Measurements with 11 mm overflow orifice

Measurement points 17-20 were done with 11 mm overflow orifice. After the particle size analysis from the particle size analyser values for d_{10}, d_{50} and d_{90} could be obtained. The collected results including solid concentration are represented in Table XIX.

Table XIX a Results of overflow for points 17 (8 mm), 18 (6 mm), 19 (5 mm) and 20 (3 mm)

Overflow						
Underflow spigot size [mm]	d10 [µm]	d50 [µm]	d90 [µm]	Mean solids [%]	STDdev [%-units]	Mean error [%-units]
8	0,864	2,94	11,1	3,35	0,03	0,02
6	0,834	2,42	7,8	3,68	0,02	0,01
5	0,849	2,56	8,01	4,11	0,09	0,05
3	0,886	2,84	8,82	4,34	1,64	0,95

Table XIX b Results of underflow for points 17 (8 mm), 18 (6 mm), 19 (5 mm) and 20 (3 mm)

Underflow						
Underflow spigot size [mm]	d10 [µm]	d50 [µm]	d90 [µm]	Mean Solids [%]	STDdev [%-units]	Mean error [%-units]
8	1,81	15,7	61,5	20,19	0,5	0,02
6	3,01	22,5	81,5	33,86	1	0,01
5	5,33	27,1	93,3	59,03	0,27	0,05
3	11,3	42,2	129	66,47	5,51	0,95

From the results can be seen that the particle size profile has changed greatly when inspecting the values of 3 mm spigot. The d-values have reduced greatly when compared to the values from 14 mm orifice. The Volumetric particle size distributions for points 17-20 are represented in Figure 24.

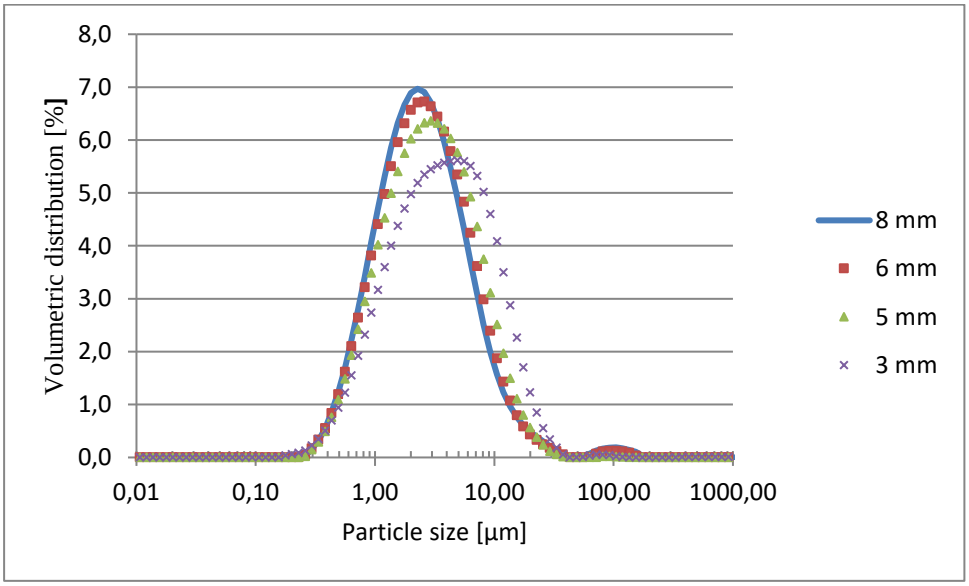

Figure 24 Volumetric particle size distribution for overflow for points 17 (8mm), 18 (6mm), 19 (5 mm) and 20 (3 mm)

As from the Figure 24 can be seen the overflow profile is different in the point of 3 mm spigot. The volumetric particle size distribution profile resembles and follows the trend of other curves as seen with measurements with high sulphur tailings.

The volumetric particle size distribution of underflow which is shown in Figure 25 can be seen the same trends as in the tests with high sulphur tailings. The peak of 3 mm spigot is normalized, and now follows the trend of when the size of underflow

spigot is reduced the distribution curve moves towards bigger particle size and their fraction from the total amount of particles in the stream is increased.

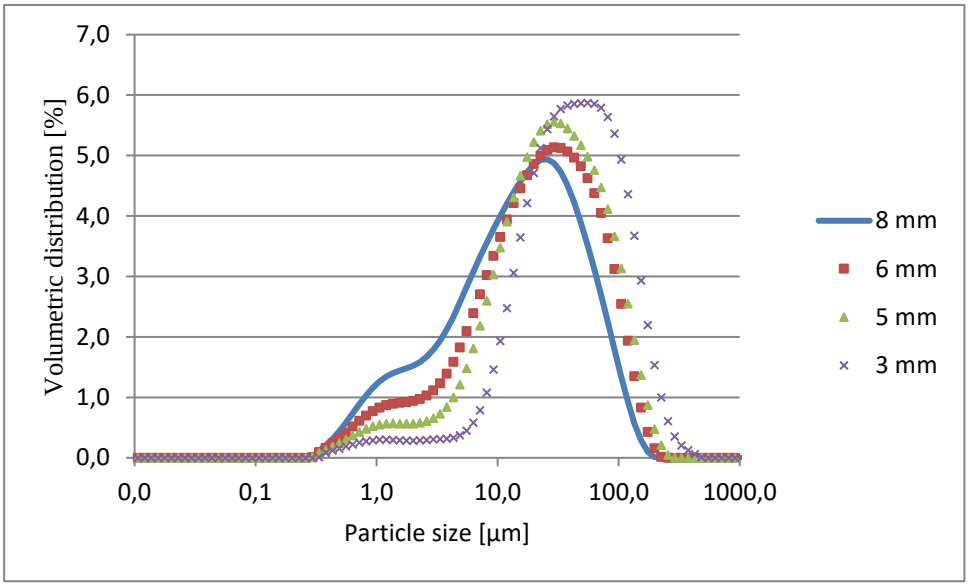

Figure 25 Volumetric particle site distribution for underflow for points 17 (8mm), 18 (6mm), 19 (5 mm) and 20 (3 mm)

Combined flowrates for over and underflow for measurement points 17 (8 mm), 18 (6 mm), 19 (5 mm) and 20 (3 mm) are represented in Table XX.

Table XX Combined flowrate results for over- and underflow for points 17 (8 mm), 18 (6 mm), 19 (5 mm) and 20 (3 mm)

Overflow				
Underflow spigot size [mm]	Mean time [s]	Mean Flow [mL/S]	STDdev [mL/s]	Mean error [mL/s]
8	5,33	384,87	22,73	10,17
6	5,03	501,29	23,49	10,50
5	4,19	492,93	22,35	10,00
3	3,98	551,14	25,52	11,41
Underflow				
Underflow spigot size [mm]	Mean time [s]	Mean Flow [mL/s]	STDdev [mL/s]	Mean error [mL/s]
8	5,33	271,12	18,02	8,06
6	5,03	169,20	5,87	2,63
5	4,19	86,99	1,83	0,82
3	3,98	53,59	2,39	1,07

Total mean flowrates: Point 17: 655,99 mL/s, point 18: 670,49 mL/s, point 19: 579,92 mL/s and point 20: 604,73.

6.3.3 Measurements with 8 mm overflow orifice

The measurement points 21-24 were carried out with the overflow orifice diameter of 8 mm. After the particle size analysis from the particle size analyser values for d_{10}, d_{50} and d_{90} could be obtained. The collected results including solid concentration are represented in Table XXI.

Table XXI Results for underflow for points 21 (8 mm), 22 (6 mm), 23 (5 mm) and 24 (2 mm)

Overflow						
Underflow spigot size [mm]	d10 [µm]	d50 [µm]	d90 [µm]	Mean solids [w-%]	STDdev [%-units]	Mean error [%-units]
8	0,78	2,08	7,83	2,51	2,19	1,26
6	0,81	2,37	7,53	2,8	0,05	0,03
5	0,84	2,62	8,21	3,29	0,24	0,14
3	0,85	2,79	8,56	3,78	0,21	0,12
Underflow						
Underflow spigot size [mm]	d10 [µm]	d50 [µm]	d90 [µm]	Mean solids [w-%]	STDdev [%-units]	Mean error [%-units]
8	1,29	9,36	39,8	12,17	0,19	1,26
6	1,64	13,5	51,4	16,56	0,73	0,03
5	3,46	26,1	94	29,89	2,05	0,14
3	7,85	39,9	141	65,59	1,2	0,12

The reduction of the size in the d-values follows the trend which was also seen in the measurements with 11 mm orifice. The volumetric particle size distribution for overflow pf measurement points 17-20 are represented in Figure 26. The particle size distribution resembles same trend in the increase of the bigger particles in the overflow as in previous measurements.

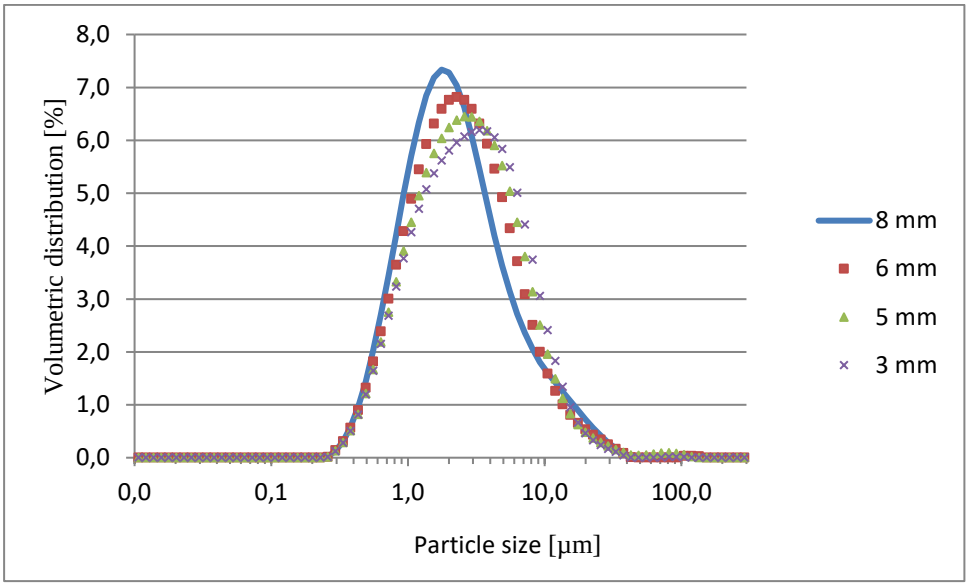

Figure 26 Volumetric particle size distribution of overflow of points 21 (8 mm), 22 (6 mm), 23 (5 mm) and 24 (2 mm)

Volumetric particle size distribution for underflow for measurement points 17-20 is represented in Figure 27.

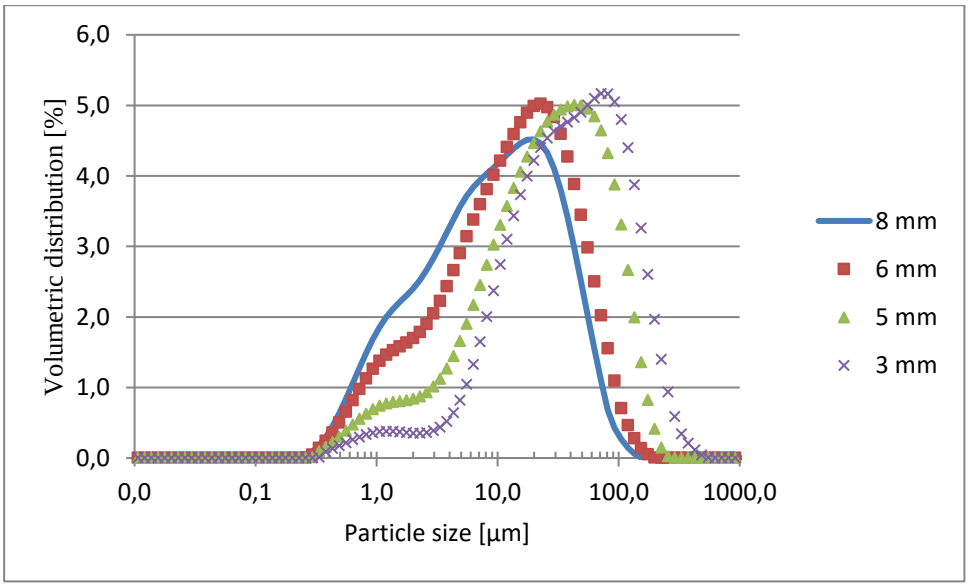

Figure 27 Volumetric particle size distribution for underflow of points 21 (8 mm), 22 (6 mm), 23 (5 mm) and 24 (2 mm)

Especially with the two smallest (5 mm and 3 mm) underflow gaps the separation is very clearly seen. Although the as with other measurement points the effect does effect on the overflow side in similar way. As from the Figure 27 can be seen points 23 and 24 seems to inhibit smaller particles entering the underflow.

Flowrates for measurement points 21-24 are represented in in Table XXII.

Table XXII Combined flowrates for measurement points 21 (8 mm), 22 (6 mm), 23 (5 mm) and 24 (2 mm)

Overflow				
Underflow spigot size [mm]	Mean time [s]	Mean Flow [mL/S]	STDdev [mL/s]	Mean error [mL/s]
8	3,60	178,51	5,51	2,46
6	5,01	256,77	8,49	3,47
5	5,17	331,13	12,04	4,92
3	3,89	400,60	24,03	10,75
Underflow				
Underflow spigot size [mm]	Mean time [s]	Mean Flow [mL/s]	STDdev [mL/s]	Mean error [mL/s]
8	3,60	350,65	10,15	4,54
6	5,01	220,46	4,93	2,01
5	5,17	128,84	8,26	3,37
3	3,89	56,70	3,07	1,37

Total flowrates: Point 21 529,16 mL/s, point 22: 477,23 mL/s, point 23: 459,97 mL/s, point 24: 457,30 mL/s.

7 CONCLUSIONS AND FURTHER STUDIES

In this study the effect of changing the geometry of the hydrocyclone was studied with two different type tailings. Two from the numerous operating parameters were chosen on which the study was based. The operating parameters that were used were the size of overflow orifice and underflow spigot. In addition for these two operating parameters hydrocyclones have other parameters which effect on the operation efficiency of the hydrocyclone. Other operating parameters were kept as constant during the test. Measurements were made for both tailings according to the research design which consisted total of 12 measurement points.

From the measurements done for both slurries could be easily be seen that changing either of the orifices had impact to the operation of the hydrocyclone. Changing the overflow orifice was noted to have very strong effect to the separation efficiency which could be seen from the shifting of the particle size distribution curve. The effect of the underflow spigot size to the separation of the particles can be seen from the results. By decreasing the underflow spigot size the particle size of the underflow increases and vice versa. This could be easily seen from particle size

distribution curves as shifting of the curves towards bigger particle size and from the increase of the solid concentration in the underflow slurry.

One of the major aspects in the operation of the hydrocyclone is the slurry and especially the solids in the slurry. In this work two different tailings were used with rather different densities. The densities were for high sulphur tailings approximately 3154 kg m^{-3} and for low sulfur tailings approximately 2907 kg m^{-3}. Also the densities for slurries were different, 1079 kg m^{-3} and 1062 kg m^{-3} low sulfur tailings slurry having lower density. For hydrocyclone to operate and work as intended there has to be density difference between the solids and the carrying liquid. Parameter that also effects on the separation process is the temperature of the carrying liquid as the temperature effects on the viscosity of the carrying liquid and by raising the temperature the solid concentration of the underflow could be raised. In this work the temperature of the slurry was not included in the list of parameters which were manipulated, but it may have had some influence on the results as there were noticeable increase in the temperature of the slurry because of the vigorous pumping and mixing of the slurry.

The importance of the properties of the slurry can also seen from the particle size distribution results. Most of the particle size distribution curves were close to each other when comparing the results from the two slurries, but some results from same configuration distinguished from each other greatly. This could be seen for example from the results of points 4 and 16, where the configuration was same, but slurry was different.

As seen from the results of the measurements done by changing only two of the geometrical operating parameters of the hydrocyclone, it is reasonable to say that hydrocyclone is effective device in solid-liquid particle separation or thickening of the slurry. In future studies more parameters should be included into the research plan. Parameters that could be included are length of the hydrocyclone, solid concentration of the slurry, temperature of the slurry and pumping pressure. Also the possibility of applying multiple hydrocyclones in series could be researched as putting hydrocyclones in series could end up into more selective separation of different sized particle fractions.

8 SUMMARY

In this work the effect of the hydrocyclone in the solid-liquid separation was made with MOZLEY C124 hydrocyclone. The Particle size distributions, solid concentrations and the sulphur concentrations of the slurries were different so two comparative studies could be made, which showed that the basic properties of the slurry have effect on certain configuration points, as results were distinguishable different. The parameters which were studied were the size of the underflow spigot D_u and the size of the vortex finder (overflow) orifice D_o.

Research design which included 12 measurement points was done and tests according to it were done to both slurries. The research design was built on the basis of available overflow orifices (3 pieces) and underflow spigots (4 pieces). At each point a total number of 3 samples were taken which were analysed resulting in total number of 72 samples. Parameters that were studied from the samples were particle size distributions and solid concentrations.

Before the measurements were done the properties of both slurries were studied. High sulphur tailings slurry had density of 1079 kg m^{-3} and solid concentration of 12,95 w-%. The density of solids in high sulfur tailings was approximately 3154 kg m^{-3}. Density of the slurry of low sulphur content was approximately 24 w-% and it had to be diluted for the tests. The diluted low sulphur slurry had solid concentration of 12,25 w-%. The density of the slurry was 1062 kg m^{-3} and the density of solids was approximately 2907 kg m^{-3}.

From the measurements could be also noted that by reducing the underflow spigot size the curve of volumetric e particle size distributions moved towards bigger particles. Opposite reaction could be seen when the overflow orifice was changed.

REFERENCES

Andrews, J.W., Gavilan Moreno, C.J., & Naorn, R.W., 2013, "Potential recovery of aluminum, titanium, lead and zinc from tailings in the abandoned Picher mining district of Oklahoma.", [Online], . Available from: http://link.springer.com/article/10.1007%2Fs13563-013-0031-7#.

Australian Government, Department of Industry, Tourism and Resources, 2007, *Tailings Management*. Available: http://www.ret.gov.au/resources/Documents/LPSDP/LPSDP-TailingsHandbook.pdf [2013, 7/16].

Choi, W.-., Lee, S.-. & Park, J.-. 2009, "Cement based solidification/stabilization of arsenic-contaminated mine tailings", *Waste Management*, vol. 29, no. 5, pp. 1766-1771.

Cilliers, J.J., Diaz-Anadon, L. & Wee, F.S. 2004, "Temperature, classification and dewatering in 10 mm hydrocyclones", *Minerals Engineering*, vol. 17, no. 5, pp. 591-597.

Coelho, M.A.Z. & Medronho, R.A. 2001, "A model for performance prediction of hydrocyclones", *Chemical Engineering Journal*, vol. 84, no. 1, pp. 7-14.

Coto, O., Galizia, F., Hernández, I., Marrero, J. & Donati, E. 2008, "Cobalt and nickel recoveries from laterite tailings by organic and inorganic bio-acids", *Hydrometallurgy*, vol. 94, no. 1–4, pp. 18-22.

Das, S.K., Kumar, S. & Ramachandrarao, P. 2000, "Exploitation of iron ore tailing for the development of ceramic tiles", *Waste Management*, vol. 20, no. 8, pp. 725-729.

Davies, M. 2011, "Filtered dry stacked tailings - The Fundementals", *Proceedings of Tailings and Mine Waste 2011*, 11/6-11/9. 7/18/2013.

Davies, M.P. & Rice, S. 2004, "An alternative to conventional tailing management – “dry stack”", [Online] 7/18/2013. Available from: http://www.infomine.com/library/publications/docs/Davies2004.pdf.

El-Shall, H. & Zhang, P. 2004, "Process for dewatering and utilization of mining wastes", *Minerals Engineering,* vol. 17, no. 2, pp. 269-277.

Firth, B. 2003, "Hydrocyclones in dewatering circuits", *Minerals Engineering,* vol. 16, no. 2, pp. 115-120.

Frachon, M. & Cilliers, J.J. 1999, "A general model for hydrocyclone partition curves", *Chemical Engineering Journal,* vol. 73, no. 1, pp. 53-59.

Franks, D.M., Boger, D.V., Côte, C.M. & Mulligan, D.R. 2011, "Sustainable development principles for the disposal of mining and mineral processing wastes", *Resources Policy,* vol. 36, no. 2, pp. 114-122.

Gunson, A.J., Klein, B., Veiga, M. & Dunbar, S. 2012, "Reducing mine water requirements", *Journal of Cleaner Production,* vol. 21, no. 1, pp. 71-82.

Heiskanen, K. 1987, *Classification handbook,* Larox, Lappeenranta.

Hernández, C.M.F., Banza, A.N. & Gock, E. 2007, "Recovery of metals from Cuban nickel tailings by leaching with organic acids followed by precipitation and magnetic separation", *Journal of hazardous materials,* vol. 139, no. 1, pp. 25-30.

Johnson, D.B. & Hallberg, K.B. 2005, "Acid mine drainage remediation options: a review", *Science of The Total Environment,* vol. 338, no. 1–2, pp. 3-14.

Kujawa, C. 2011, "Cycloning of Tailing for the Production of Sand as TSF Construction Material", *Tailings and mine waste 2011*, 11/6-11/9.

Lottermoser, B.G. 2010, *Mine Wastes: Characterization, Treatment and Environmental Impacts,* 3rd ed. Springer-Verlag Berlin and Heidelberg GmbH & Co. KG.

Lutandula, M.S. & Maloba, B. 2013, "Recovery of cobalt and copper through reprocessing of tailings from flotation of oxidised ores", *Journal of Environmental Chemical Engineering,* vol. 1, no. 4, pp. 1085-1090.

Martin, T.E., Davies M.P., Rice, S., Higgs T & Lighthall P.C. "Stewardship of tailings facilities", [Online], . Available from: http://pebblescience.org/pdfs/tailings_stewardship-1.pdf.

Mudd, G.M., Weng, Z., Jowitt, S.M., Turnbull, I.D. & Graedel, T.E. 2013, "Quantifying the recoverable resources of by-product metals: The case of cobalt", *Ore Geology Reviews,* vol. 55, pp. 87-98.

Muravyov, M.I., Fomchenko, N.V., Usoltsev, A.V., Vasilyev, E.A. & Kondrat'eva, T.F. 2012, "Leaching of copper and zinc from copper converter slag flotation tailings using H_2SO_4 and biologically generated $Fe_2(SO_4)_3$", *Hydrometallurgy,* vol. 119–120, pp. 40-46.

Nageswararao, K., Wiseman, D.M. & Napier-Munn, T.J. 2004, "Two empirical hydrocyclone models revisited", *Minerals Engineering,* vol. 17, no. 5, pp. 671-687.

Neesse, T., Dueck, J. & Minkov, L. 2004, "Separation of finest particles in hydrocyclones", *Minerals Engineering,* vol. 17, no. 5, pp. 689-696.

Northey, S., Mohr, S., Mudd, G.M., Weng, Z. & Giurco, D. 2014, "Modelling future copper ore grade decline based on a detailed assessment of copper resources and mining", *Resources, Conservation and Recycling,* vol. 83, pp. 190-201.

Richardson, J.F., J.F. Richardson, J.H. Harker & J.R. Backhurst 2002, *Coulson and Richardson's chemical engineering : Particle technology and separation processes. Volume 2,* 5th ed.,Revised edn, Butterworth Heinemann.

Sinnott, R.K. 2005, *Coulson and Richardson's chemical engineering : Chemical engineering design. Volume 6,* 4th ed.,Revised edn, Butterworth-Heinemann.

Svarovsky, L. 1981., *Solid-liquid separation,*, Butterworths, London.

Svarovsky, L. 1984, *Hydrocyclones,* Holt, Rinehart and Winston, London.

Tavares, L.M., Souza, L.L.G., Lima, J.R.B. & Possa, M.V. 2002, "Modeling classification in small-diameter hydrocyclones under variable rheological conditions", *Minerals Engineering,* vol. 15, no. 8, pp. 613-622.

Wills, B.A. 2006., *Will's mineral processing technology : : an introduction to the practical aspects of ore treatment and mineral recovery /,* Oxford :, Elsevier/Butterworth-Heinemann,.

Yan, D., Parker, T. & Ryan, S. 2003, "Dewatering of fine slurries by the Kalgoorlie Filter Pipe", *Minerals Engineering*, vol. 16, no. 3, pp. 283-289.

Zagury, G.J., Oudjehani, K. & Deschênes, L. 2004, "Characterization and availability of cyanide in solid mine tailings from gold extraction plants", *Science of The Total Environment*, vol. 320, no. 2–3, pp. 211-224.

APPENDICES

APPENDIX I Results from preliminary tests of high and low sulphuric tailing slurries.

Solid content for high sulphur tailing slurry

Sample	Cup Mass [g]	Wet mass [g]	Dry mass [g]	Solids [%]
1	7,2	211,03	28,74	13,62
2	7,24	194,42	24,7	12,70
3	6,97	165,33	20,8	12,58
Average				12,96809
STDdev				0,567008
Mean error				0,327362

Density measurements for high sulphur tailing slurry

V [ml]	Mass [g]	Density [kg/m3]
37	40,47	1093,784
53	57,57	1086,226
56	60,24	1075,714
63	68	1079,365
74	77,79	1051,216
77	83,34	1082,338
83	90,21	1086,867
85	91,78	1079,765
Mean		1079,409
STDdev		12,68255
Meanerror		4,010575

Solid concentration for low sulphur tailings slurry

Sample	Cup mass [g}	Wet mass [g]	Dry mass [g]	Solids [%]
1	7,01	266,86	40,14	12,41475
2	7,05	245,03	36,65	12,08015
3	6,97	224,17	36,66	13,24441
4	7,01	262,34	36,59	11,27544
Mean				12,25369
STDdev				0,815384
Mean error				0,407692

Density of the low sulphur tailings slurry

Volume [mL]	Mass [g]	Density [kg/m3]
66	70,24	1064,242
76	79,83	1050,395
78	84,86	1087,949
83	88,21	1062,771
84	87,84	1045,714
Mean		1062,214
STDdev		16,4213
Mean error		7,343828

APPENDIX II Measurement data from the tests with high sulphur tailings slurry

Solid contents from under- and overflows from high sulphur tailings slurry

Measurement point	Cup mass UF [g]	Cup mass OF [g]	Wet mass UF [g]	Wet mass OF [g]
1	2,24	2,23	93,85	80,65
	2,24	2,17	105,8	64,99
	2,2	2,22	109,49	80,28
2	2,23	2,22	123,34	83,02
	2,23	2,23	93,77	115,36
	2,22	2,24	148,14	97,33
3	2,25	2,25	44,01	46,43
	2,22	2,24	45,26	55,81
	2,14	2,21	24,69	26,94
4	2,15	2,22	77,21	40,41
	2,18	2,22	74,52	56,15
	2,18	2,22	71,76	54,29
5	2,22	na.	25,39	na.
	2,18	2,2	36,1	56,52
	2,18	2,18	23,33	40,62
6	2,18	2,21	48	33,41
	2,2	2,21	34	30,61
	2,21	2,2	36,58	57,95
7	2,21	2,18	40,7	38,46
	2,2	2,22	35,96	29,33
	2,21	2,2	17,89	35,48
8	2,2	2,21	45,95	55,01
	2,2	2,17	18,42	71,33
	2,19	2,19	17,33	58,32
9	2,24	2,25	46,55	36,92
	2,24	2,21	52,23	32,6
	2,21	2,24	41,66	49,04
10	2,22	2,23	50,37	61,52
	2,22	2,22	57,66	70,04
	2,17	0,74	53,03	13,95
11	0,72	0,73	20,33	28,57
	0,72	0,73	25,29	23,09
	0,72	0,73	15,84	25,55
12	0,72	0,72	14,99	21,63
	0,73	0,73	18,84	27,1
	0,74	0,73	20,11	27,73

Solid contents from under- and overflows from high sulphur tailings slurry

Measurement point	Dry mass UF [g]	Dry mass OF	Solid UF [%]	Solid OF [%]
1	32,07	8,22	31,78	7,43
	41,6	7,06	37,2	7,52
	42,85	8,22	37,13	7,47
2	59,48	8,34	46,42	7,37
	45,81	10,62	46,48	7,27
	85,38	9,57	56,14	7,53
3	27,07	5,56	56,4	7,13
	27,03	6,3	54,82	7,27
	9,59	4,34	30,17	7,91
4	8,37	5,55	8,06	8,24
	8,22	6,84	8,11	8,23
	7,97	6,74	8,07	8,33
5	8,51	na.	24,77	na.
	9,39	5,53	19,97	5,89
	7,82	4,64	24,17	6,06
6	16,32	4,25	29,46	6,11
	12,4	4,04	30	5,98
	13,29	5,83	30,29	6,26
7	19,94	4,61	43,56	6,32
	18,34	4,14	44,88	6,55
	9,48	4,51	40,64	6,51
8	32,94	6,25	66,9	7,34
	14,23	7,46	65,31	7,42
	13,52	6,44	65,38	7,29
9	7,81	3,96	11,97	4,63
	8,5	3,71	11,99	4,6
	7,18	4,49	11,93	4,59
10	9,66	5,34	14,77	5,06
	10,75	5,81	14,79	5,13
	9,99	1,44	14,75	5,02
11	4,72	2,46	19,68	6,06
	5,65	2,07	19,49	5,8
	3,83	2,2	19,63	5,75
12	7,26	2,12	43,63	6,47
	8,68	2,47	42,2	6,42
	9,22	2,54	42,17	6,53

Averages, standard error, and mean error for the results of solid content measurements of the under- and overflows of high sulphur tailings slurry

Measurement point	Mean UF [%]	Mean OF [%]	STDdev UF [-]	STDdev OF [-]	Mean error UF [-]	Mean error OF [-]
1	35,37	7,48	3,11	0,05	1,793	0,03
2	49,68	7,39	5,59	0,13	0,075	0,08
3	47,13	7,44	14,70	0,41	0,239	0,24
4	69,23	8,26	-	0,05	-	0,03
5	22,97	5,97	2,62	0,12	1,850	0,08
6	29,92	6,12	0,42	0,14	0,244	0,08
7	43,03	6,46	2,17	0,12	1,255	0,07
8	65,86	7,35	0,90	0,06	0,519	0,04
9	11,96	4,61	0,03	0,02	0,016	0,01
10	14,77	5,07	0,02	0,05	0,014	0,03
11	19,60	5,87	0,10	0,16	0,055	0,09
12	42,66	6,47	0,84	0,05	0,482	0,03

Table XXIII Densities for under and overflows from high sulphur slurry.

Measurement point	Volume UF [mL]	Volume OF [mL]	Mass UF [g]	Mass OF [g]	Density UF [kg/dm3]	Density OF [kg/dm3]
1	49	74	65,69	76,35	1,341	1,032
	71	56	94,30	57,68	1,328	1,030
2	38	97	53,49	99,22	1,408	1,023
	65	64	92,79	65,48	1,428	1,023
3	59	81,5	94,00	83,59	1,593	1,026
	59	89	92,79	91,14	1,573	1,024
4	18	67	33,33	83,59	1,852	1,248
	60	94	93,45	91,14	1,558	0,970
5	34,5	59	39,89	59,36	1,160	1,01
	63	59	72,77	61,56	1,160	1,04
6	54	59	65,46	61,29	1,210	1,040
	59	59	72,18	61,08	1,220	1,040
	39	59	55,28	59,5	1,417	1,01
7	67	59	94,30	60,74	1,407	1,03
		59		60,64		1,028
8	22	59	37,22	61,8	1,692	1,047
		59		61,83		1,048
	59	59	62,73	60,64	1,063	1,028
9	59	59	62,68	61,8	1,062	1,047
	59	59	63,58	60,41	1,078	1,024
	59	59	62,73	59,38	1,063	1,006
10	59	59	65,33	60	1,107	1,017
	59	59	66,11	60,58	1,121	1,027
	59	59	67,52	61,06	1,144	1,035
11	59	59	67,01	59,61	1,136	1,010
	22	59	27,78	58,94	1,263	0,999
	14	59	16,53	60,66	1,181	1,028
12	21	59	26,95	59,79	1,283	1,013
	22	59	27,78	58,94	1,263	0,999

Average density, standard deviation and mean error for the density measurements of the under- and overflow from high sulphur slurry

Measurement point	Mean UF	Mean OF	STDdev UF	STDdev OF	Mean error UF	Mean error OF
1	1,334	1,031	0,009	0,001	0,006	0,001
2	1,418	1,023	0,014	0,000	0,010	0,000
3	1,583	1,025	0,015	0,001	0,010	0,001
4	1,705	1,109	0,208	0,197	0,147	0,139
5	1,160	1,025	0,000	0,021	0,000	0,015
6	1,215	1,040	0,007	0,000	0,005	0,000
7	1,412	1,020	0,007	0,014	0,005	0,008
8	1,692	1,041	-	0,012		0,007
9	1,068	1,033	0,009	0,013	0,005	0,007
10	1,097	1,017	0,030	0,010	0,017	0,006
11	1,181	1,015	0,071	0,018	0,041	0,011
12	1,242	1,014	0,054	0,015	0,031	0,008

Flowrates for under-. and overflow from high sulphur slurry. Pointss number 1-6.

Measurement point	Time [s]	Underflow [ml]	Overflow [ml]	Q(UF) [mL/s]	Q(OF) [mL/s]	Q(tot) [L/s]
	3,53	700,00	2250,00	198,30	637,39	0,84
	3,91	790,00	2450,00	202,05	626,60	0,83
1	4,38	900,00	2750,00	205,48	627,85	0,83
	4,00	890,00	2700,00	222,50	675,00	0,90
	4,42	900,00	3000,00	203,62	678,73	0,88
	3,55	310,00	2600,00	87,32	732,39	0,82
	3,98	370,00	2850,00	92,96	716,08	0,81
2	3,41	330,00	2650,00	96,77	777,13	0,87
	2,91	280,00	2225,00	96,22	764,60	0,86
	3,59	340,00	2800,00	94,71	779,94	0,87
	1,76	80,00	1350,00	45,45	767,05	0,81
3	1,56	70,00	1200,00	44,87	769,23	0,81
	1,50	60,00	970,00	40,00	646,67	0,69
	3,46	70,00	2950,00	20,23	852,60	0,87
	4,19	87,50	3225,00	20,88	769,69	0,79
4	3,83	80,00	2900,00	20,89	757,18	0,78
	3,15	70,00	2500,00	22,22	793,65	0,82
	3,86	90,00	3000,00	23,32	777,20	0,80
		1600,00	2200,00			
	5,12	1550,00	2100,00	302,73	410,16	0,71
5	5,79	1700,00	2450,00	293,61	423,14	0,72
	5,09	1550,00	2050,00	304,52	402,75	0,71
	5,12	740,00	2500,00	144,53	488,28	0,63
	4,79	660,00	2250,00	137,79	469,73	0,61
6	4,60	640,00	2500,00	139,13	543,48	0,68
	4,66	700,00	2300,00	150,21	493,56	0,64
	4,73	720,00	2500,00	152,22	528,54	0,68

Flowrates for under-. and overflow fromhigh sulphur slurry. Points number 7-12.

Measurement point	Time [s]	Underflow [ml]	Overflow [ml]	Q(UF) [mL/s]	Q(OF) [mL/s]	Q(tot) [L/s]
	2,40	180,00	1340,00	75,00	558,33	0,63
	2,29	160,00	1260,00	69,87	550,22	0,62
7	2,25	150,00	1200,00	66,67	533,33	0,60
	2,47	180,00	1340,00	72,87	542,51	0,62
	2,11	160,00	1220,00	75,83	578,20	0,65
	4,87	130,00	3100,00	26,69	636,55	0,66
	4,91	120,00	2900,00	24,44	590,63	0,62
8	5,10	140,00	3200,00	27,45	627,45	0,65
	5,27	140,00	3300,00	26,57	626,19	0,65
	5,58	150,00	3250,00	26,88	582,44	0,61
	5,34	2100,00	1100,00	393,26	205,99	0,60
	5,49	2200,00	1100,00	400,73	200,36	0,60
9	5,55	2200,00	1100,00	396,40	198,20	0,59
	5,11	1900,00	950,00	371,82	185,91	0,56
	4,34	1100,00	800,00	253,46	184,33	0,44
	5,46	1300,00	1500,00	238,10	274,73	0,51
	7,54	1250,00	2050,00	165,78	271,88	0,44
10	7,49	1700,00	2000,00	226,97	267,02	0,49
	8,47	1900,00	2300,00	224,32	271,55	0,50
	7,56	1800,00	2100,00	238,10	277,78	0,52
	6,13	1500,00	1750,00	244,70	285,48	0,53
	6,12	750,00	2000,00	122,55	245,10	0,37
	3,60	400,00	1150,00	111,11	569,44	0,68
11	3,24	380,00	1120,00	117,28	617,28	0,73
	3,25	380,00	1150,00	116,92	707,69	0,82
	3,66	410,00	1200,00	112,02	573,77	0,69
	3,69	440,00	1220,00	119,24	474,25	0,59
	3,26	130,00	1400,00	39,88	613,50	0,65
	4,07	150,00	1640,00	36,86	282,56	0,32
12	3,53	140,00	1500,00	39,66	317,28	0,36
	3,14	130,00	1400,00	41,40	366,24	0,41
	3,41	130,00	1440,00	38,12	351,91	0,39

Averaga flowrate, standard deviation and mean error for the flowrate measurements of the high sulphur slurry

Measurement point	Mean time	Mean Flow UF [mL/s]	Mean Flow OF [mL/S]	STDdev UF	STDdev OF	Mean error UF	Mean error OF	Total mean flow [mL/s]
1	4,05	206,39	649,11	9,39	25,71	4,20	11,50	855,50
2	3,49	93,60	754,03	3,81	28,40	1,70	12,70	847,62
3	1,61	43,44	727,65	2,99	70,14	1,73	40,49	771,09
4	3,70	21,51	790,06	1,24	37,37	0,56	16,71	811,57
5	5,36	298,61	409,93	5,84	9,40	2,61	4,21	708,54
6	4,78	144,78	504,72	6,44	30,37	2,88	13,58	649,49
7	2,30	72,05	552,52	3,79	17,08	1,69	7,64	624,57
8	5,15	26,41	612,65	1,15	24,35	0,51	10,89	639,06
9	5,17	363,13	194,96	62,31	9,44	27,87	4,22	558,09
10	7,11	223,00	274,74	29,05	6,36	11,86	2,60	497,74
11	3,93	116,52	531,26	4,34	159,33	1,77	65,05	647,78
12	3,48	39,18	386,30	1,74	131,08	0,78	58,62	425,48

APPENDIX III Measurement data from low sulphur tailings slurry

Solid contents from under- and overflows from low sulphur tailings slurry

Measurement point	Cup mass [g]	Mass Wet UF [g]	Mass Wet OF [g]	Mass Dry UF [g]	Mass Dry OF [g]	Solid UF [%]	Solid OF [%]
	0,73	15,72	16,49	5,83	1,34	32,44	3,70
13	0,73	13,83	13,46	5,28	1,25	32,90	3,86
	0,73	20,79	20,71	7,52	1,52	32,66	3,81
	0,73	35,5	20,44	19,56	1,56	53,04	4,06
14	0,73	30,94	20,14	17,4	1,55	53,88	4,07
	0,73	31,6	22,03	16,62	1,62	50,28	4,04
	0,73	32,33	13,49	23,88	1,32	71,61	4,37
15	0,73	51	18,66	37,8	1,54	72,69	4,34
	0,73	33,51	23,62	25,12	1,73	72,78	4,23
	0,73	32,07	33,25	24,82	3,41	75,12	8,06
16	0,73	29,91	22,32	22,58	2,51	73,05	7,97
	0,73	30,41	19	22,94	2,19	73,04	7,68
	0,73	19,19	21,78	4,55	1,46	19,91	3,35
17	0,73	16,03	22,9	3,92	1,49	19,90	3,32
	0,73	25,33	29,28	5,99	1,72	20,77	3,38
	0,73	22,55	24,97	8,48	1,65	34,37	3,68
18	0,73	21,74	20,22	8,23	1,47	34,50	3,66
	0,73	20,21	26,84	7,34	1,72	32,71	3,69
	0,73	20,38	17,64	12,82	1,47	59,32	4,20
19	0,73	29,65	23,63	18,22	1,7	58,99	4,10
	0,73	20,65	28,39	12,87	1,87	58,79	4,02
	0,73	27,39	18,36	21,08	1,71	74,30	5,34
20	0,73	30,55	42,9	26,34	1,78	83,83	2,45
	0,73	42,9	22,36	32,6	1,9	74,29	5,23
	0,73	23,62	18,24	3,56	1,21	11,98	2,63
21	0,73	15,6	16,3	2,63	1,13	12,18	2,45
	0,73	16,84	11,88	2,81	1,02	12,35	2,44
	0,73	31,68	16,82	5,84	1,21	16,13	2,85
22	0,73	14,98	26,24	3,15	1,46	16,15	2,78
	0,73	17,98	25,66	3,86	1,44	17,41	2,77
	0,73	18,49	18,09	6,38	1,3	30,56	3,15
23	0,73	30,02	21,61	9,01	1,41	27,58	3,15
	0,73	21	21,85	7,35	1,51	31,52	3,57
	0,73	35,32	17,9	23,43	1,38	64,27	3,63
24	0,73	49,34	28,22	33,59	1,77	66,60	3,69
	0,73	37,8	19,2	25,64	1,5	65,90	4,01

Average solid content, standard deviation and mean error for the solid concentration measurements from the under- and overflows of low sulphur tailings slurry.

Measurement point	Mean solids UF [%]	Mean solids OF [%]	STDdev UF [%-units]	STDdev OF [-]	Mean error UF [-]	Mean error OF [-]
13	32,67	3,79	0,23	0,08	0,132	0,05
14	52,40	4,06	1,88	0,02	0,009	0,01
15	72,36	4,32	0,65	0,07	0,042	0,04
16	73,73	7,91	1,20	0,20	0,114	0,11
17	73,73	3,35	0,50	0,03	0,018	0,02
18	33,86	3,68	1,00	0,02	0,009	0,01
19	59,03	4,11	0,27	0,09	0,052	0,05
20	77,47	4,34	5,51	1,64	0,946	0,95
21	12,17	2,51	0,19	2,19	1,262	1,26
22	16,56	2,80	0,73	0,05	0,027	0,03
23	29,89	3,29	2,05	0,24	0,140	0,14
24	65,59	3,78	1,20	0,21	0,118	0,12

Slurry density for under and overflows from low sulphur tailings slurry

Measurement point	Volume [mL]	Mass UF [g]	Mass OF [g]	Density UF [kg/dm^{-3}]	Density OF [kg/dm^{-3}]
	59,00	73,75	61,70	1,250	1,046
13	59,00	75,04	59,52	1,272	1,009
	59,00	74,20	60,23	1,258	1,021
	59,00	92,99	59,28	1,576	1,005
14	59,00	90,90	59,40	1,541	1,007
	59,00	91,13	58,75	1,545	0,996
	59,00	114,67	59,07	1,944	1,001
15	59,00	115,75	59,20	1,962	1,003
	59,00	115,20	58,77	1,953	0,996
	59,00	117,07	50,99	1,984	0,864
16	59,00	116,61	60,37	1,976	1,023
	59,00	117,50	60,60	1,992	1,027
	59,00	60,10	59,43	1,019	1,007
17	59,00	67,14	60,75	1,138	1,030
	59,00	67,20	58,50	1,139	0,992
	59,00	74,50	59,63	1,263	1,011
18	59,00	73,54	58,68	1,246	0,995
	59,00	74,05	58,59	1,255	0,993
	59,00	98,02	60,15	1,661	1,019
19	59,00	97,62	60,12	1,655	1,019
	59,00	98,50	60,80	1,669	1,031
	59,00	120,45	59,74	2,042	1,013
20	59,00	118,05	61,24	2,001	1,038
	59,00	119,77	61,39	2,030	1,041
	59,00	62,81	60,12	1,065	1,019
21	59,00	63,06	60,05	1,069	1,018
	59,00	62,70	60,22	1,063	1,021
	59,00	65,56	60,30	1,111	1,022
22	59,00	66,49	59,75	1,127	1,013
	59,00	66,85	59,24	1,133	1,004
	59,00	72,28	59,59	1,225	1,010
23	59,00	73,67	59,39	1,249	1,007
	59,00	75,42	59,40	1,278	1,007
	59,00	104,23	58,61	1,767	0,993
24	59,00	105,00	58,65	1,780	0,994
	59,00	104,80	58,40	1,776	0,990

Flowrates for Under and overflow from low sulphur tailings slurry. Points number 13-18.

Set	Time [s]	Underflow [mL]	Overflow [mL]	Q(UF) [mL/s]	Q(OF) [mL/s]	Q(tot) [L/s]
13	3,78	800,00	2350	211,64	621,69	0,83
	3,9	800	2300	205,13	589,74	0,79
	5,03	1050	3100	208,75	616,30	0,83
	6,22	1300	3650	209,00	586,82	0,80
14	2,82	360	2150	127,66	762,41	0,89
	2	260	1500	130,00	750,00	0,88
	1,78	230	1340	129,21	752,81	0,88
	2,15	300	1600	139,53	744,19	0,88
15	2,62	190	1700	72,52	648,85	0,72
	1,91	150	1400	78,53	732,98	0,81
	1,78	150	1400	84,27	786,52	0,87
	1,66	140	1275	84,34	768,07	0,85
16	1,63	120	1550	73,62	950,92	1,02
	1,66	140	1520	84,34	915,66	1,00
	1,38	120	1240	86,96	898,55	0,99
	2,00	160	1600	80,00	800,00	0,88
17	6,03	1500	2200	248,76	364,84	0,61
	5,16	1400	1900	271,32	368,22	0,64
	5,34	1450	2100	271,54	393,26	0,66
	4,78	1400	1975	292,89	413,18	0,71
18	4,5	800	2400	177,78	533,33	0,71
	5,38	900	2600	167,29	483,27	0,65
	4,56	750	2300	164,47	504,39	0,67
	5,68	950	2750	167,25	484,15	0,65

Flowrates for Under and overflow from low sulphur tailings slurry. Points number 19-24.

Measurement point	Time [s]	Underflow [mL]	Overflow [mL]	Q(UF) [mL/s]	Q(OF) [mL/s]	Q(tot) [L/s]
19	4,75	420	2450	88,42	515,79	0,60
	4,56	400	2250	87,72	493,42	0,58
	4,00	350	1850	87,50	462,50	0,55
	3,44	290	1720	84,30	500,00	0,58
20	4,66	250	2600	53,65	557,94	0,61
	3,81	200	2150	52,49	564,30	0,62
	3,34	190	1900	56,89	568,86	0,63
	4,09	210	2100	51,34	513,45	0,56
21	2,68	920	500	343,28	186,57	0,53
	4,25	1550	740	364,71	174,12	0,54
	3,06	1050	540	343,14	176,47	0,52
	4,41	1550	780	351,47	176,87	0,53
22	5,72	1280	1500	223,78	262,24	0,49
	4,38	980	1150	223,74	262,56	0,49
	5,43	1200	1400	220,99	257,83	0,48
	4,5	960	1100	213,33	244,44	0,46
23	6,97	820	2200	117,65	315,64	0,43
	4,5	600	1550	133,33	344,44	0,48
	5,16	660	1700	127,91	329,46	0,46
	4,03	550	1350	136,48	334,99	0,47
24	3,59	220	1560	61,28	434,54	0,50
	3,78	210	1500	55,56	396,83	0,45
	4,53	250	1780	55,19	392,94	0,45
	3,65	200	1380	54,79	378,08	0,43

Calculated Average flowrates, standard deviation and mean error for the measurements from low sulphur tailings slurry

Measurement point	Mean time	Mean Flow UF [mL/s]	Mean Flow OF [mL/S]	STDdev UF [-]	STDdev OF [-]	Mean error UF [-]	Mean error OF [-]	Total mean flow [mL/s]
13	4,73	208,63	603,64	2,68	17,91	1,34	8,96	812,27
14	2,19	131,60	752,35	5,38	7,61	2,40	3,40	883,95
15	1,99	79,92	734,11	5,63	61,02	3,25	35,23	814,02
16	1,67	81,23	891,28	5,83	64,64	2,61	28,91	972,51
17	5,33	271,12	384,87	18,02	22,73	8,06	10,17	656,00
18	5,03	169,20	501,29	5,87	23,49	2,63	10,50	670,48
19	4,19	86,99	492,93	1,83	22,35	0,82	10,00	579,91
20	3,98	53,59	551,14	2,39	25,52	1,07	11,41	604,73
21	3,60	350,65	178,51	10,15	5,51	4,54	2,46	529,16
22	5,01	220,46	256,77	4,93	8,49	2,01	3,47	477,23
23	5,17	128,84	331,13	8,26	12,04	3,37	4,92	459,97
24	3,89	56,70	400,60	3,07	24,03	1,37	10,75	457,30

APPENDIX IV Example of use of equations (5.1) - (5.3).

Determination of mass concentration for the solids in SFC slurry

$$C_w = \frac{m_s}{m_{sl}} = \frac{30{,}11\,g}{120{,}34} = 0{,}250$$

Determination of slurry concentration

$$\rho_{sl} = \frac{m_{sl}}{V_{sl}} = \frac{0{,}12034\,kg}{10^{-4}\,m^3} = 1203{,}4\,\frac{kg}{m^3}$$

Determination of solid true density

$$\rho_s = \frac{\rho_{sl} C_w \rho_L}{\rho_L - \rho_{sl}(1 - C_w)} = \frac{1203{,}4\,\frac{kg}{m^3} \cdot 0{,}250 \cdot 0{,}9977\,\frac{kg}{m^3}}{0{,}9977\,\frac{kg}{m^3} - 1203{,}4\,\frac{kg}{m^3}(1 - 0{,}250)} = 3154{,}58\,\frac{kg}{m^3}$$

For low sulphur tailings slurry following starting values were used

$m_s = 28{,}57\,g$
$m_{sl} = 118{,}47\,g$

By using these values with same V_{sl} and ρ_L values density of the solids in FT slurry was 2906,56 kg m^{-3}.